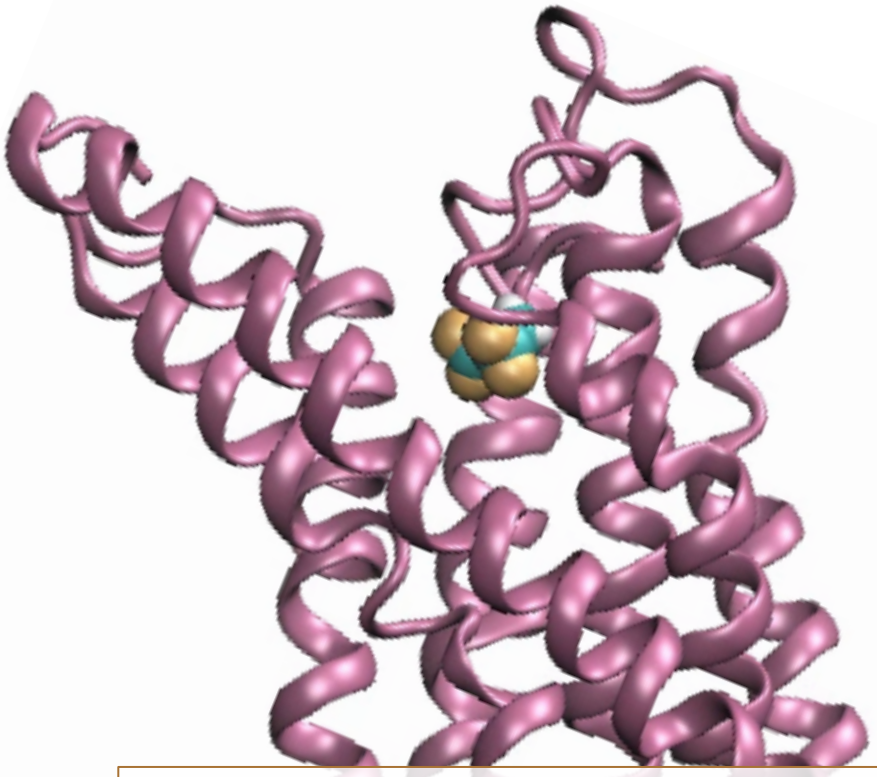

The differential signalling of the succinate receptor SUCNR1/GPR91, through Gi versus Gq

Master thesis – Sofie Liljewall

Faculty of Engineering, LTH, Lund University

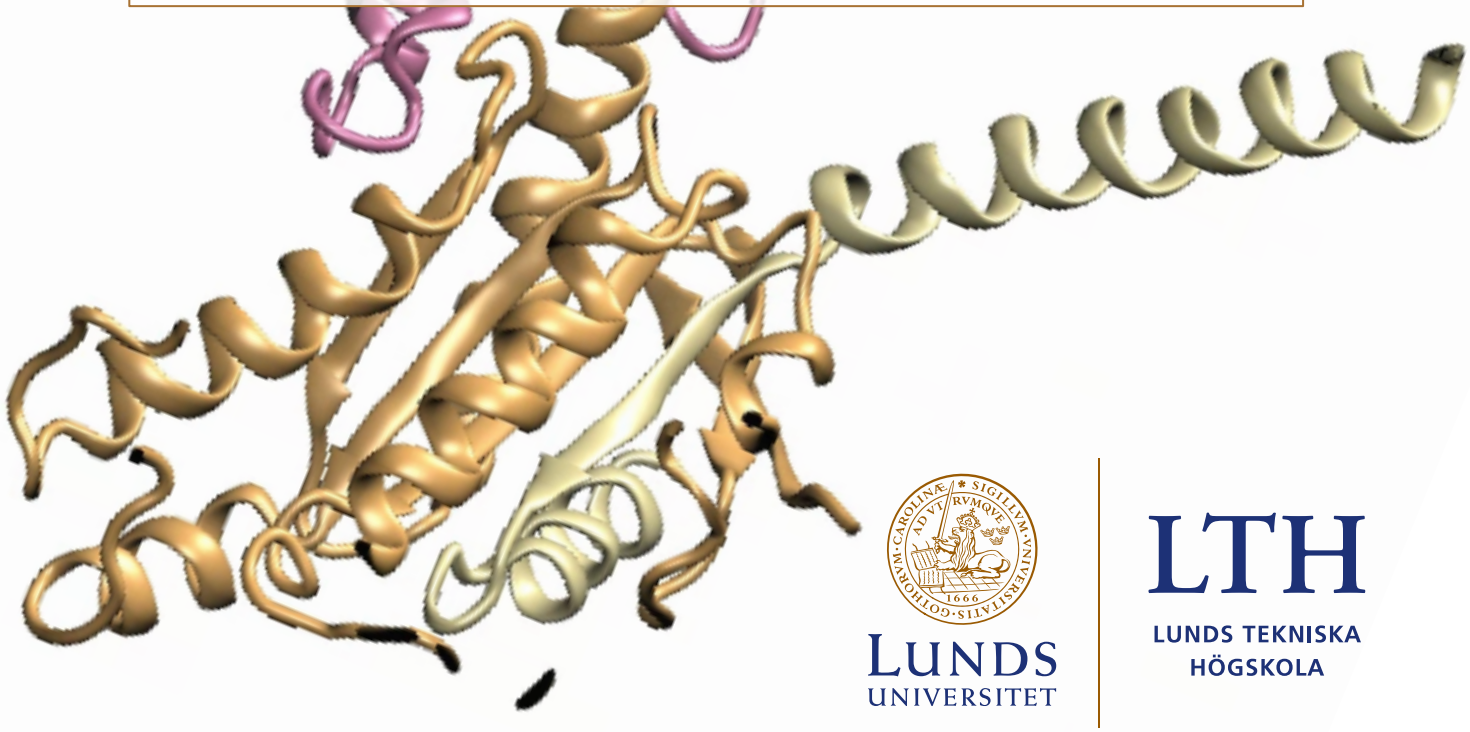

LUNDS UNIVERSITET

LTH
LUNDS TEKNISKA HÖGSKOLA

The differential signalling of the succinate receptor SUCNR1/GPR91, through Gi versus Gq

Master's degree project in Applied Microbiology, KMBM05
Faculty of Engineering, LTH, Lund University

Sofie Liljewall

2022-06-13

Project executed with the Schwartz group at Novo Nordisk Foundation Center for Basic Metabolic Research (CBMR), University of Copenhagen

Supervisor at LTH
Jenny Schelin

Examiner
Magnus Carlquist

Supervisors at CBMR
PhD student Jacob E. Petersen
Postdoc Mette Trauelsen
Professor Thue W. Schwartz

Key words: GPR91, SUCNR1, G protein recruitment, Gi, Gq, TRUPATH biosensor, BRET2

Front page: Model of mGPR91 coupled to Gi alpha subunit. Credit: Aslihan Shenol Illiyaz, PhD student at CBMR.

Acknowledgements

First and foremost, I want to thank Jacob for being the absolute best supervisor one could possibly ask for. Thank you for always answering my questions, for teaching me everything I needed to know, and for all the laughs. Writing this thesis have been a great pleasure and I look forward to continuing working together.

I would like to thank Thue for taking a chance on a Swedish engineer and letting me in as a part of your group. And for your support and valuable input and discussions throughout my project.

Also, a big thanks to Mette for always helping with your great knowledge and discussions whenever I got stuck and needed guidance. And to Asli for your expert help with everything related to structural analysis, alignments, and data analysis.

Also, a big thanks to the entire Schwartz group for instantly welcoming me and making me feel like a part of the group. You are all amazing!

A big thanks to Jenny, for always looking out for my best and all your valuable feedback on my work throughout the entirety of this project.

Finally, I would also like to thank my mentor, Thomas. Thank you for all your advice, and for being a good discussion partner. It is safe to say that this thesis would not have been what it is without you.

Abstract

G protein-coupled receptors are the biggest family of membrane bound receptor in the human genome, they are also target for many drugs due to their accessible location in the cell membrane. We have characterized the G protein recruitment of the succinate receptor 1 (SUCNR1/GPR91). GPR91 was deorphanized in 2004 and already then it was suggested that GPR91 could couple to the Gi-family and the Gq-family of G proteins. Since then, the fact that it could do this have been debated. We have used and optimized the TRUPATH biosensor (Olsen et al., 2020) to show dose-response recruitment curves for both hGPR91 and mGPR91 for the Gi- and Gq-family of G proteins. We show that hGPR91 recruits all tested α-subunits of the Gi- and Gq-family whilst mGPR91 recruits all except for αQ. We also show that mGPR91 is approximately 1 order more potent than hGPR91. We conclude that the TRUPATH biosensor is a good tool for investigation of G protein recruitment, but it needs to be optimized to fit each receptor that should be investigated. Further on we suggest using the results obtained as a guide for further investigation of GPR91 structurally as well as to see if there is any bias signaling occurring.

Table of contents

Introduction

Key ingredients when trying to understand how and why a disease progresses and when eventually finding a treatment or drug are to understand WHAT is happening in the diseased cells and WHY it is happening. Many diseases are a result of when signalling within or between cells goes wrong. Our bodies signalling molecules are often collectively referred to as ligands, and the amplifier of these signals are called receptors. Receptors are proteins located anywhere in the cell and they are key communicators within and between cells. When talking about ligands, one usually looks at one of two different types; agonists, which are activators of the receptor, and antagonists, which work the opposite of the agonist. The receptor in focus in this thesis is the G protein-coupled receptor 91 (GPR91), also known as the succinate receptor 1 (SUCNR1). The name succinate receptor 1 comes from the main agonist (endogenous ligand) that communicates via this receptor, succinate. Succinate is an intermediate in the citric acid cycle that is a key energy producing pathway in our bodies.

Signalling via GPR91 plays important roles in several tissues such as kidney, liver, and heart and is involved in diseases in these tissues. In this thesis, I investigate and characterize the signalling properties of GPR91. This is a knowledge that is important to be able to further investigate new treatments for diseases where GPR91 is involved, by targeting GPR91.

Aim

The aim of this thesis is to:

- Implement and optimize the TRUPATH biosensor in mammalian cells.
- Substantiate the finding that GPR91 is recruiting/signalling via different G protein families (Gi and Gq).
- Investigate the difference between recruitment/signalling within the Gi- and Gq-family for both human and murine GPR91.
- Show dose-response curves for succinate for both human and murine GPR91, with Gi- and Gq-family coupling.

Background

G protein-coupled receptors

The superfamily

G protein-coupled receptors, GPCRs, is the largest family of membrane bound receptors in the human body present in many different cell types and tissues (Fredriksson et al., 2003). This superfamily consists of more than 800 receptors and are classified into different families. There are two different classifications used within GPCRs, which are the International Union of Pharmacology's (IUPHAR) classifications (Table 1), which is based on sequence homology and considers both vertebrates and invertebrates, where class D and E are specific for invertebrates, and the GRAFS system (Table 2), that is based on phylogenetic origin and only considers vertebrates (de Francesco et al., 2017).

Table 1. The IUPHAR's classification of GPCRs (de Francesco et al., 2017).

Class	A	B	C	D	E	F
Name	Rhodopsin-like	Secretin-like	Metabotropic/ Glutamate	Fungal mating receptors	Cyclic nucleotide receptors	Frizzled/ smoothened
% of all GPCRS	85.5 %	7 %	3.81 %	0.45 %	0.38 %	2.84 %

Table 2. The GRAFS-system GPCR classification (de Francesco et al., 2017).

Class	G	R	A	F	S
Name	Glutamate-family	Rhodopsin-family	Adhesion-family	Frizzled/taste 2- family	Secretin-family
No. of members	22	710	33	11	15

Below follows a brief description of each family of the GRAFS classification. The glutamate-family have a long N-termini that forms a Venus fly trap structure, with the ligand binding to the cavity. Glutamate is a neurotransmitter that is present in the brain in humans. Some examples of receptors are glutamate receptors, GABA receptors and taste receptors. The secretin-family and the adhesion-family are structurally similar; therefore, they are clumped together as Class B in the IUPHAR classification. They both have an N-termini that is rich with cysteine residues. The secretin-family have a long N-termini (60-80 amino acid residues) where large peptide ligands bind. The adhesion-family, which also have a long N-termini also often have a lot of Ser and Thr residues. The signalling via secretin-family receptors is often paracrine. Looking at the frizzled/taste 2-family the frizzled receptors are involved in cell fate such as cell growth, proliferation, and polarity whilst the taste 2 receptors are not very known but are believed to be expressed on the tongue and be involved in bitter taste reception. All the above-mentioned families are considered to have long N-termini that are essential for ligand binding. The rhodopsin family, which is by far the largest family, and the one of interest in this thesis, instead has a relatively short N-termini and the ligands instead bind in cavities between the TMs. The ligands that bind to the rhodopsin-family receptors varies greatly, with ligands such as hormones, neuropeptides, and light (Schiöth & Fredriksson, 2005).

GPCRs play a crucial role in the human body, being responsible for example for hormone and neurotransmitter signalling, cell growth and differentiation, immune response as well as our vision, olfaction, and taste (Rosenbaum et al., 2009). It is thereby safe to say that GPCRs are very central players in mammalian cells.

Because of their very accessible location in the cellular membrane, see Figure 1, they are also key drug targets for the pharmaceutical industry. In 2018 Hauser and co-workers showed, that 108 different GPCRs were the targets for approximately 34 % of all FDA approved drugs (Hauser et al., 2018). Some examples of drugs that target GPCRs are Levodopa (for Parkinson's disease), Lorazepam (for anxiety), Chloroquine (for malaria) and many more (Sriram & Insel, 2018).

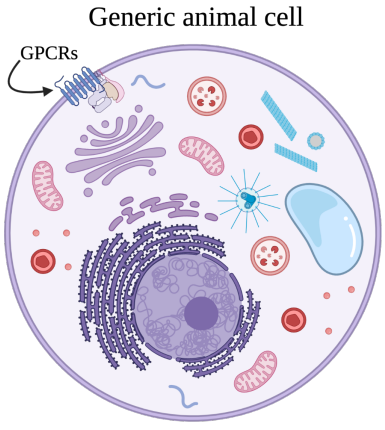

Figure 1. General structure of an animal cell showing the placement of GPCRs in the cellular membrane in relation to the rest of the cell structure. Figure created with BioRender.com.

Structure

The main characteristic for all the GPCRs is their structure. They all consist of seven transmembrane helices (7TMs), connected by intracellular and extracellular loops as well as an intracellular C-terminus and an extracellular N-terminus (Rosenbaum et al., 2009). Figure 2 shows a schematic representation of the general GPCR structure. The first GPCR structure to ever be solved was rhodopsin in complex with 11-cis retinol (Palczewski et al., 2000) using cryo-electron microscopy and biochemical data. Since the structural characterization of rhodopsin that served as a useful template, together with developments of protein engineering methods as well as the technical developments of x-ray crystallography several GPCR structures have been solved and is found in the Protein Data Bank (PDB) (Zhang et al., 2015). Interestingly, as can be found in the GPCR databank (gpcrdb.org) is that there are many different structures for the same receptor, indicating the flexibility of GPCRs.

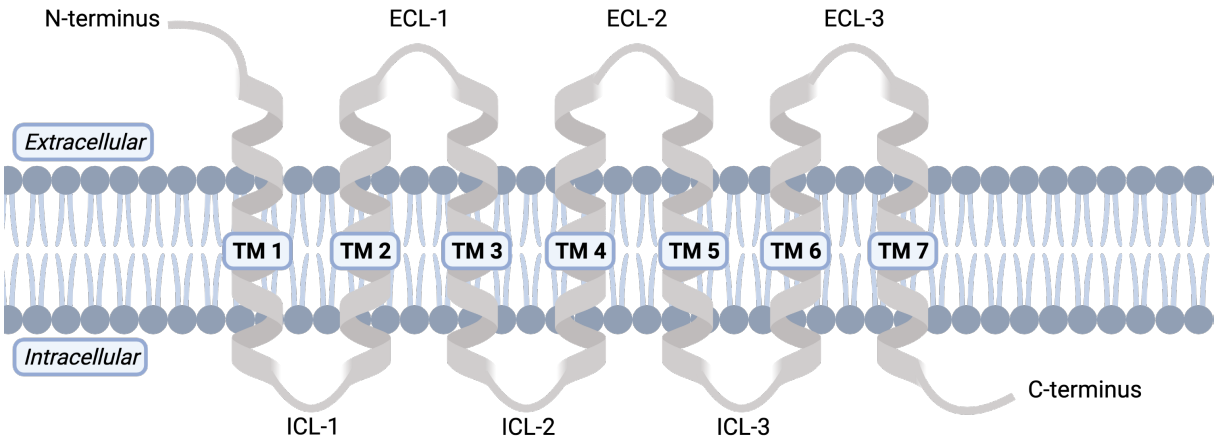

Figure 2. A schematic illustration of the main components of a general GPCR structure. The TM's are transmembrane helixes that span over the cellular membrane these are connected to one another by intra- and extra-cellular loops (ICL and ECL), the N-terminus of the receptor is on the extracellular part of the cell and the C-terminus on the intracellular side, Figure created with BioRender.com.

G proteins

As mentioned previously and as is indicated by their name, GPCRs couple to G proteins intracellularly as part of their signalling mechanism. G proteins are heterotrimeric proteins consisting of an α, β, and γ subunit. In its inactive state the three subunits form a heterotrimer, however, once a ligand binds the receptor the trimer dissociates to form an α-complex and a βγ-complex. Depending on what G protein the GPCR is coupled to/recruits it signals in different ways (Neves et al., 2002).

Signalling

The signalling of GPCRs is mediated by several different types of ligands, for example metabolites, hormones, neurotransmitters, chemokines and many more. The signalling of GPCRs can be described as a signalling cascade since it is done in multiple steps where one protein activates another, and second messengers are utilized. There are four different G proteins classified according to the α-subunit, $G\alpha_s$, $G\alpha_{i/o}$, $G\alpha_{q/11}$ and $G\alpha_{12/13}$, that all have different signalling pathways (Neves et al., 2002) for a summary of the different alpha subunits that belongs to each family, see Table 3. The different signalling classifications will further be referred to as Gs, Gi, Gq and G12/13.

Table 3. Summary of the different α-subunits in each signalling family.

Gs	Gi	Gq	G12/13
αsS, αsL, αOlf	αi1, αi2, αi3, αoA, αoB, αz, αGust	αQ, α11, α14, α15, α16	α12, α13

The general starting position for the signalling is the inactive state of the G protein where the α-subunit is bound to GDP and associated with the βγ-dimer. Upon receptor activation (i.e. ligand binds to the receptor) the G protein trimer gets involved by GDP dissociation from Gα, quickly GTP is instead bound to the Gα (due to the high intercellular concentration of GTP). The binding of GTP to the nucleotide binding site induces a conformational change of the Gα subunit that results in the dissociation of the G protein trimer, forming separate Gα subunit and a Gβγ subunit. Both parts of the dissociated G protein can then further mediate different signalling in the cell. The signalling is terminated by the hydrolysis of GTP to GDP and the re-association of the Gα subunit with the Gβγ subunit forming the inactive heterotrimer (Hilger et al., 2018). Below follows a brief description of the different signalling pathways by the different α-subunits.

The **Gαs** subunit activates the effector adenylyl cyclase, AC. AC then catalyses the formation of the second messenger cyclic adenosine monophosphate, cAMP, from ATP. cAMP binds protein kinase A, PKA, making PKA release its catalytic subunits. The catalytic subunits of PKA are then part of regulating numerous proteins by phosphorylation. The **Gαi** subunit mediates the opposite signal than Gαs. It inhibits the activation of AC and thus the entire cAMP pathway by not making it possible to convert ATP to cAMP (Rosenbaum et al., 2009). For a schematic overview, see Figure 3.

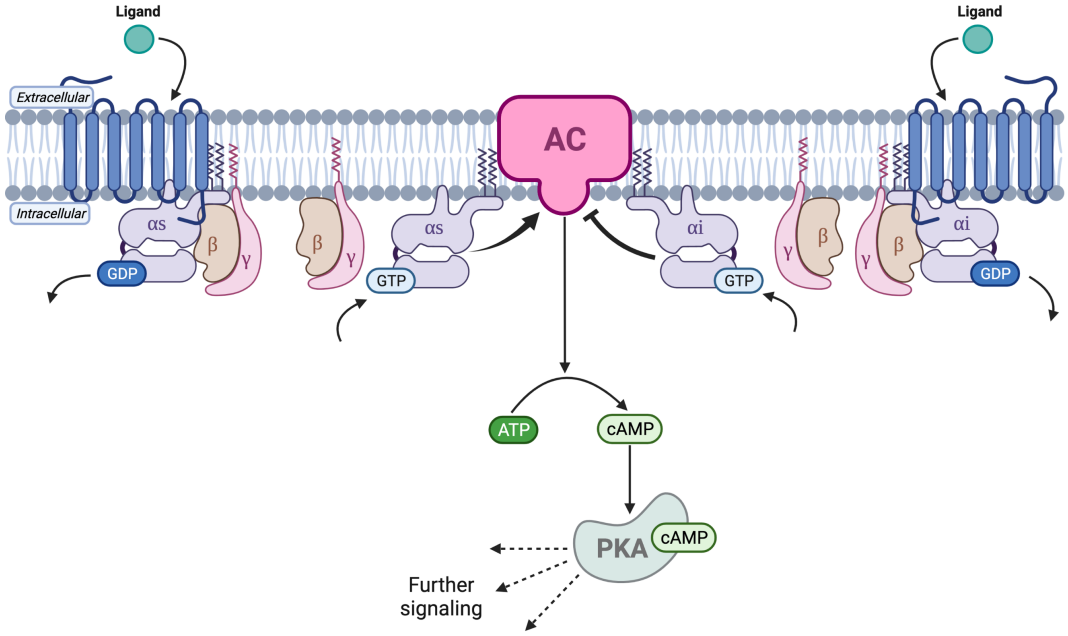

Figure 3. Schematic overview of the Gαs (left) and Gαi (right) signalling pathways. Ligand binding the GPCR recruits the trimeric G protein, GDP is exchanged for GTP which leads to a conformational change of the alpha subunit which dissociates the trimeric structure to form the single alpha subunit and a dimeric beta-gamma subunit. The lone alpha subunit will activate (Gαs) or inhibit (Gαi) AC. The activated AC will convert ATP to cAMP that will activate PKA. PKA will then signal further downstream in the cell. GPCR – G protein-coupled receptor, GDP – guanosine diphosphate, GTP – guanosine triphosphate, AC – adenylyl cyclase, cAMP – cyclic adenosine monophosphate, PKA – protein kinase A. Figure created with BioRender.com.

The **Gαq** subunit activates phospholipase C, PLC. The activated PLC then cleaves PIP_2 to form the second messengers IP_3 and DAG. IP_3 binds to IP_3 gated calcium channels in the ER which releases Ca^{2+} in the cell. Ca^{2+} also acts as a second messenger activating various proteins and thus many different cellular responses. DAG is left bound to the intracellular part of the cell membrane, and it will bind to and activate protein kinase C, PKC. PKC will then signal further by its phosphorylation properties (Rosenbaum et al., 2009). For a schematic overview see Figure 4.

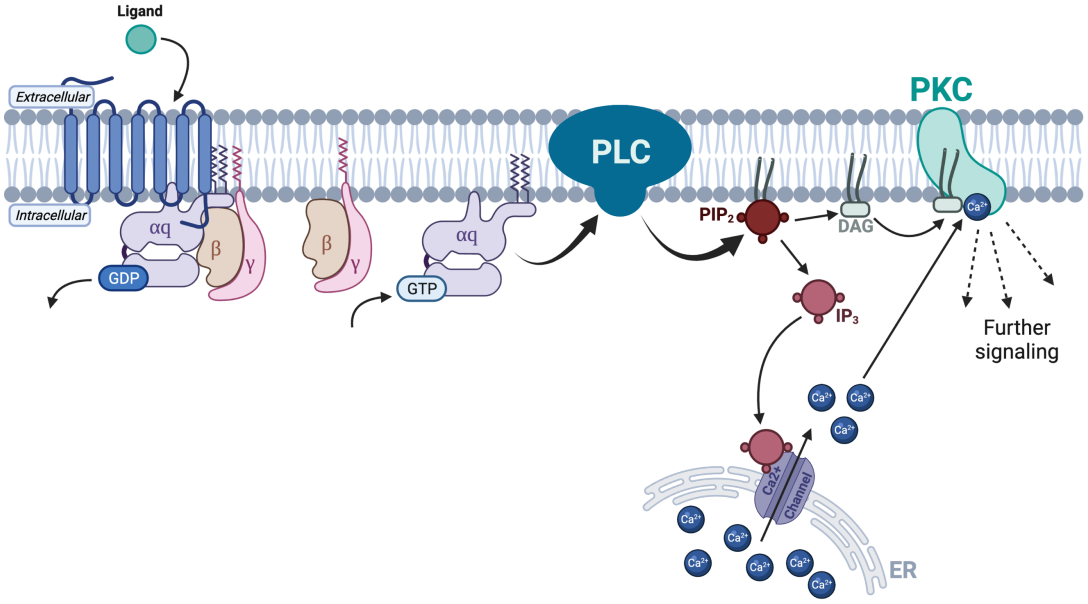

Figure 4. Schematic overview of the Gαq mediated signalling pathway. Ligand binding the GPCR recruits the trimeric G protein, GDP is exchanged for GTP which leads to a conformational change of the alpha subunit which dissociates the trimeric structure to form the single alpha subunit and a dimeric beta-gamma subunit. The lone alpha subunit will activate PLC that then cleaves PIP2 to DAG and IP3. IP3 will bind Ca2+ channels in the ER and thus releasing Ca2+ intracellularly. IP3 and DAG will also interact with PKC that further signals downstream in the cell.
GPCR – G protein-coupled receptor, GDP – guanosine diphosphate, GTP – guanosine triphosphate, PLC – phospholipase C, PIP2 - Phosphatidylinositol 4,5-bisphosphate, IP3 - Inositol trisphosphate, DAG – Diacyl glycerol, Ca2+ - Calcium ions, ER – endoplasmic reticulum, PKC – protein kinase C. Figure created with BioRender.com.

The **Gα12/13** subunit signalling is the least explored signalling pathway, this is mainly due to that they do not activate any easily measurable second messengers. The Gα12/13 subunit recruits' translocation of the inactive RhoGEFs (guanine nucleotide exchange factor (GEF) for the Rho family of GTPases) from the cytosol to the cell membrane. RhoGEFs have GAP (GTPase-activating protein) activity towards the Gα12/13, stimulating its GEF activity, which then mediates downstream activation of the GTPase RhoA. RhoA then further regulate several downstream effectors (Worzfeld et al., 2008).

The "turnoff" mechanism of GPCR signalling involves two key participants, the G protein coupled receptor kinases (GKRs) and arrestins. The first step involves the activated GPCRs βγ-subunit that recruits GKRs to the membrane where they phosphorylate the activated GPCR which initially halts the coupling of more G proteins to the receptor but does not shut of the signalling completely. Further on, arrestins are recruited as they bind to the GPCR with higher affinity than the G proteins, thus terminating the signalling fully (Gurevich & Gurevich, 2019).

Both GKRs and arrestins can also signal independently of GPCRs (Gurevich & Gurevich, 2019), this will however not be a central concept of this thesis.

Bias signalling

Another important concept about GPCR coupling and signalling is that one receptor can couple to different G proteins thus resulting in different intracellular signalling by the same receptor. This concept, known as bias signalling, is central for this thesis. There are several aspects that affect biased signalling, the ligand, the receptor itself and the transducers (e.g., G proteins). As an example, a ligand binds to the receptor, which induces a conformational change, this conformational change then affects the affinity of the G protein intracellularly, this is known as ligand bias. There is also the concept of receptor bias, where a mutated version of the receptor differs in comparison to the wild type (WT) receptor. Lastly, there is also what is called system bias. System bias is when the signalling is affected because of an excess expression of a specific transducer (Smith et al., 2018).

The alpha-subunits

As presented in Table 3 there are several different alpha-subunits in each signalling family. The main difference between the alpha-subunits within the same family is in what tissue/cell type they are expressed. Below follows a summary of the different alpha-subunit families:

Gas-family

The Gαs-family consists of two members. The name in parenthesis after each member states what gene encodes that specific protein, αs (GNAS) and αOlf (GNAL). αs is detected in all human tissues and have low tissue specificity (Human Protein Atlas – GNAS). αOlf is detected in many tissues but is enriched in the brain (Human Protein Atlas – GNAL).

Gai-family

There are five members of the Gαi-family. The name in parenthesis after each member states what gene encodes that specific protein, αi1(GNAI1), αi2 (GNAI2), αi3 (GNAI3), αo (GNAO1) and αz (GNAZ). αi1 is expressed in all human tissues and has low tissue specificity (Human Protein Atlas – GNAI1). αi2 and αi3 are all detected in all or close to all tissues in humans and have low tissue specificity, αi2 is enhanced in the skin and adipose tissue (Human Protein Atlas – GNAI2, GNAI3). αo is detected in several different tissues but is specific mainly in the brain and the retina (Human Protein Atlas – GNAO1). αo also has two different isoforms, these are called αoA and αoB, the two different isoforms have a 94.4 % sequence identity (Uniprot – GNAO1). The last member is αz, it is also detected in many different tissues but is mainly enhanced in the brain (Human Protein Atlas – GNAZ).

Gaq-family

The Gαq-family consists of αQ (GNAQ), α11 (GNA11), α14 (GNA14), α15 (GNA15) and α16 (GNA16). αQ, α11, and α14 is detected in all (or nearly all) tissues and have a low tissue specificity, αQ is most highly expressed in the brain and bone marrow and α11 is most highly expressed in the gastrointestinal tract, muscles and in the male and female reproductive system (Human Protein Atlas – GNAQ, GNA11, GNA14). α15 and α16 are detected in many tissues but are enhanced in bone marrow and oesophagus (Human Protein Atlas – GNA15, GNA16).

Gα12/13-family

The Gα12/13 family consists of α12 (GNA12) and α13 (GNA13). α12 is detected in all tissues and has low tissue specificity. It is most highly expressed in the brain (Human Protein Atlas – GNA12). α13 is also detected in all human tissues but is enhanced in the bone marrow and lymphoid tissues (Human Protein Atlas – GNA13).

TCA-cycle

As mentioned in the introduction, the ligand for the receptor of interest (GPR91) in this thesis is succinate, an intermediate in the tricarboxylic citric acid cycle (TCA-cycle). The TCA-cycle, also called the Krebs cycle and the citric acid cycle, is a metabolic pathway that is the most important source of energy for cells as well as central part of the aerobic respiration. For a schematic overview of the TCA-cycle and its connection with the electron transport chain (ETC), see Figure 5. The TCA cycle consists of a series of chemical reactions mediated by specific enzymes where the starting substrate, Acetyl-CoA, originates from the breakdown of glucose. It produces energy in the form of GTP as well as indirectly by NADH and $FADH_2$ that are electron carriers in the ETC. As such, the TCA-cycle is tightly linked with the ETC. The ETC requires oxygen and is the cells mechanism for ATP production. The ETC consists of five protein complexes and some helper molecules located in the inner mitochondrial membrane. The ETC creates a proton gradient by transferring H^+ ions over the inner mitochondrial membrane. This proton gradient is then used to drive the fifth complex, ATP-synthase, forming ATP (Martínez-Reyes & Chandel, 2020).

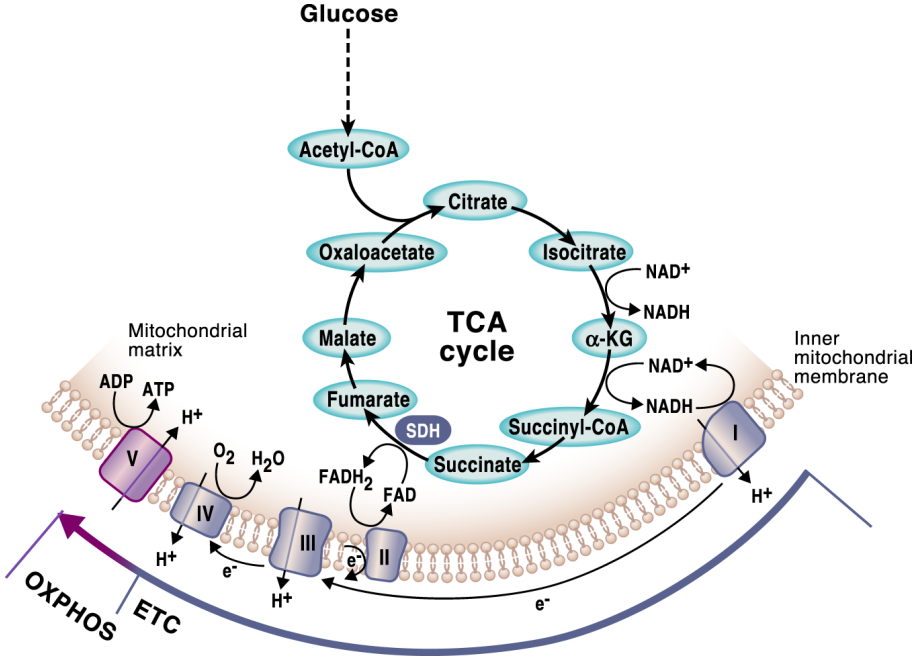

Figure 5. Schematic overview of the TCA-cycle and its connection with the ETC. Acetyl-CoA enters the TCA-cycle and forms together with oxaloacetate citrate, citrate is then converted to isocitrate which when it is converted to alpha ketoglutarate also forms NADH from NAD+. α ketoglutarate is then converted to succinyl-CoA, also forming NADH from NAD+. The formed NADHs "enters" the ETC by releasing its H+ to complex I located in the inner mitochondrial membrane. Succinyl-CoA is converted to succinate that is then converted to fumarate (by succinate dehydrogenase), in this step FAD is reduced to FADH2 which interacts with ETC complex II (succinate dehydrogenase). Fumarate is converted to malate that is converted to oxaloacetate that together with a new Acetyl-CoA forms citrate and the cycle goes on. The rest of the complexes in the ETC pumps H+ over the inner mitochondrial membrane, creating a membrane potential that complex V, ATP synthase, utilizes as its driving force to form ATP from ADP. Figure borrowed from (Martínez-Reyes & Chandel, 2020). Abbreviations: ETC – electron transport chain, OXPHOS – oxidative phosphorylation, SDH – succinate dehydrogenase, complex I - NADH ubiquinone oxidoreductase, complex II – succinate dehydrogenase, complex III - coenzyme Q: cytochrome c – oxidoreductase, complex IV - cytochrome c oxidase, complex V – ATP synthase.

Succinate dehydrogenase

When the cells are under normal physiological conditions (i.e., atmospheric oxygen concentration, glucose concentration between 1-20 mM, no disease that affects for example the metabolism etc.), the TCA cycle moves along as the name suggests, as a cycle, with no accumulations of any intermediates. When the cells experience stress, such as hypoxia or hyperglycaemia, the ETC and TCA-cycle no longer function as normal. One effect is on the enzyme succinate dehydrogenase (SDH), making it act in the reverse direction, reducing fumarate to succinate, leading to an accumulation of succinate (Chouchani et al., 2014). High levels of succinate, both intracellularly and systemically have been linked to several physiological effects. This will be addressed in later sections.

The GPR91/SUCNR1 receptor

Signalling

The investigated receptor in this thesis is the G protein-coupled receptor 91, GPR91 or as it is also called the succinate receptor 1, SUCNR1. GPR91 is a part of the rhodopsin-family. GPR91 was deorphanized in 2004 (He et al., 2004) when its endogenous ligand was discovered to be the TCA-cycle intermediate succinate. Trauelsen and colleagues has later shown that several compounds from the TCA-cycle as well as synthetic succinate analogues can in fact bind and activate GPR91, however, not with the same potency and efficacy as succinate (Trauelsen et al., 2017a).

Originally, it was shown that GPR91 signals through the recruitment of both Gi and Gq (He et al., 2004). The claim about Gq coupling was then argued to be attributed to the PLC-β activation by the βγ-dimer (Gilissen et al., 2016). However, in 2021, Trauelsen and colleagues presented that hyperpolarization of M2 macrophages by extracellular succinate is mediated through GPR91 Gq signalling (Trauelsen et al., 2021) confirming that GPR91 with certainty can couple both Gi and Gq and thus demonstrating different signalling/amplifying properties depending on the type of G protein coupled to the receptor.

However, there is still a lot to learn about the signalling properties of GPR91. It is not yet established what determines the Gi versus Gq coupling, and how it differs between different cell types, tissues, and species. As mentioned earlier, this is crucial knowledge when trying to understand a specific diseases progression, and how to be able to treat it. The work done in this thesis is aimed at getting further understanding of these GPR91 properties.

GPR91's interaction with G proteins

The parts of GPR91 that interact with the α-subunit of the G protein are the ICL-2 and ICL-3 as well as TM-I, TM-VI and TM-VII (Latorraca et al., 2017). The part of the G protein alpha-subunit that interacts with the GPCR is the C-termini and the amino acids in proximity to the C-termini, called the G-alpha 5 helix (Liu et al., 2020; Xia et al., 2021).

Expression (tissues/cell types)

The GPR91 is expressed in several different tissues/cell types. Below follows a brief description of some of the different tissues in which GPR91 is expressed as well as its main signalling properties. A common in denominator regarding research about GPR91 is that the actual signalling

mechanism is hardly ever mentioned. If this is just because the authors do not deem it important or if it is not recognized, remains unknown.

Kidney

GPR91 is highly expressed in the kidneys and more precisely in the juxtaglomerular apparatus (JGA). He and colleagues showed this by qRT-PCR expression analysis in 2004. They also showed that GPR91 seems to be the receptor responsible for succinate-induced hypertension, by activation of the renin – angiotensin system, RAS (He et al., 2004). These findings were seconded in 2009 when Vargas and colleagues pinpointed by RT-PCR and immunohistochemistry what cell type in the JGA that were expressing GPR91. The only cell type in the JGA that expressed GPR91 was the macula densa (MD) cells. As mentioned earlier accumulation of succinate is a signal of metabolic stress. In this state GPR91 in MD cells are shown to activate MAPKs, COX-2 and mediate the release of prostaglandin E_2, all of which can be coupled to the activation of RAS (Vargas et al., 2009).

The RAS is the human system for regulating blood pressure. Low blood pressure is recognized by the JGA in the kidneys, which releases renin. Renin then cleaves angiotensinogen to form angiotensin I, which is then converted by ACE to form angiotensin II that is involved in several mechanisms to increase blood pressure.

GPR91 is also expressed in the luminal membrane of tubular cells (He et al., 2004) and in the glomerular endothelial cells. However, the physiological role remains unknown (Fernández-Veledo et al., 2021).

Liver

In the liver GPR91 is expressed in quiescent hepatic stellate cells (HSC). It has been shown that hepatic ischemia results in a significant increase of succinate. The increase of succinate in the liver leads to maturation of the HSC via paracrine GPR91 activation. Activation of HSC is the livers defence mechanism against damage. Looking at the different GPCR mediated signalling pathways, there is no observed signalling of Gi nor Gq in HSC (Correa et al., 2007).

Later research has also shown that the above mechanism can also lead to liver inflammation and fibrosis (Mills et al., 2021).

White adipose

GPR91's role in white adipose tissue (in mice) was presented by Regard and co-workers in 2008. They showed that extracellular succinate signalling via GPR91 seems to inhibit lipolysis in a dose-dependent fashion with an IC50 value of 44 μM. They also state that it is likely that the signalling is Gi-coupled since other Gi-coupled GPCRs are known to inhibit lipolysis in adipose tissue (Regard et al., 2008). Lipolysis is the process where lipid triglycerides are hydrolysed to form glycerol and three fatty acids. Lipolysis is an important metabolic pathway with its main purpose to quickly mobilize energy.

Retina

As mentioned, succinate accumulates because of hypoxia. In the retina, GPR91 is located in the ganglion cell layer (GCL). Here it plays a crucial role in mediating several pro-angiogenic factors responsible for neovascularization in response to the high levels of accumulated succinate. The mechanism of secondary angiogenesis/neovascularization is well known to be a key mechanism in the pathological aspect of different retinopathic diseases (Sapieha et al., 2008).

Brain

GPR91 is found mainly in the neurons in the cerebral cortex. There it has been shown, much like its role in the retina, to be involved in angiogenesis and the stimulation of pro-angiogenic factors such as VEGF (Chemtob et al., 2013).

Heart

In the heart, GPR91 is located on cardiomyocytes, the heart muscle cells. There it has been shown to signal via two different pathways in the response to high levels of extracellular succinate. Firstly, it is shown to activate MAPKs and secondly, to activate PLC that then further signals intracellularly. Both these signalling events relates to cardiomyocyte hypertrophy, the increase of heart-muscle cell size and enhanced protein production, a condition that can be fatal (de Castro Fonseca et al., 2016).

Bone marrow

In human bone marrow GPR91 has been identified in CD34+ progenitor cells, megakaryocyte progenitor cell cultures, erythroid progenitor cell cultures as well as in bone marrow-derived stromal cell cultures and TF-1 cells. Stimulation with succinate on both megakaryocyte progenitor cell cultures and erythroid progenitor cell cultures increased the growth and proliferation of these. To obtain a deeper understanding of the signalling mechanism of cell proliferation by succinate stimulation, Hakak and colleagues used the cell line TF-1 and identified that succinate with GPR91 would signal via the Gi pathway and then further activate the MAPK-Erk pathway. However, the MAPK-Erk pathway is allegedly activated by the βγ-subunit and not by the αi-subunit. Hakak and colleagues also showed that succinate would protect TF-1 cells from serum-starvation induced cell death as well as the recovery of multilineage blood cells in myelosuppression induced by chemotherapy (Hakak et al., 2009).

Blood

In the blood GPR91 has been detected in megakaryocytes, platelets, T-cells, B-cells, and monocytes (Macaulay et al., 2006), dendritic cells and macrophages (Rubic et al., 2008).

GPR91 and cancer

Recently there is a growing interest in understanding cancer metabolism and the function of metabolites in cancer progression/regulation. Tumour cells are reprogrammed to utilize accumulating metabolites to their own advantage and one of these metabolites is succinate. Succinate is known to promote tumour growth, and as succinate accumulates the expression of GPR91 is upregulated. It is not yet established any direct link between GPR91 and cancer, but the fact that succinate is a well-known oncometabolite, and that signalling via GPR91 is known to promote angiogenesis, tissue fibrosis and inflammation it is likely that GPR91 acts as a tumour cell

promotor. (Ristic et al., 2017) It has also been shown that tumours release succinate and through GPR91 signals to polarize macrophages into tumour-associated macrophages (TAM) promoting tumour growth and metastasis. (Wu et al., 2020)

TRUPATH – BRET^2

One major part of this thesis consists of applying and optimizing the TRUPATH biosensor platform. A schematic overview of the TRUPATH mechanism is presented in Figure 6. Below follows a description of the technical background and mechanism of this. TUPATH is a biosensor platform for investigation of the GPCR transducerome (collective term for all G proteins that couple to GPCRs) (Olsen et al., 2020). It consists of plasmids coding for 14 different alpha subunits, 2 different beta subunits and 4 different gamma subunits. The alpha subunits are conjugated with the bioluminescent protein *Renilla* luciferase (RLuc8) and the gamma subunits with green fluorescent protein (GFP2). The mechanism utilized to measure agonist-induced trimer dissociation (GPCR signalling) is BRET (Bioluminescence Resonance Energy Transfer) (Olsen et al., 2020).

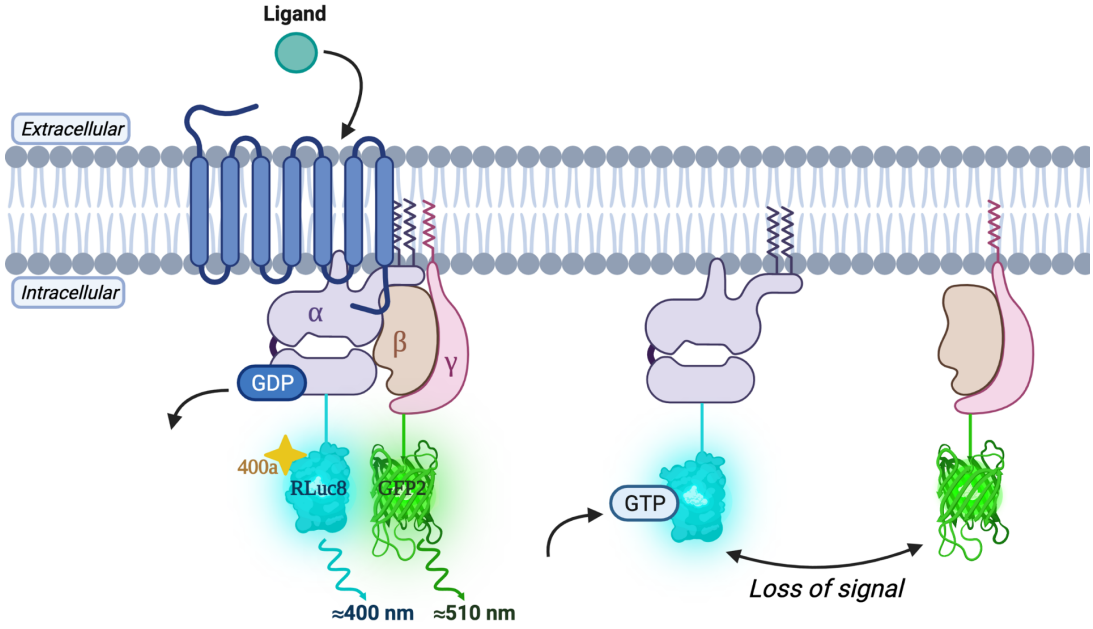

Figure 6. Schematic overview of the TRUPATH mechanism. The substrate Coelenterazine 400a (400a in figure) activates RLuc8, that emits light, the proximity of GFP2 to RLuc8 allows for GFP2 to emit light. Ligand binding initiates signalling by the exchange of GDP to GTP and dissociation of heterotrimer to α-complex and βγ-complex, this results in loss of signal from GFP2 du to that it is no longer close enough to RLuc8 to be able to emit light. This is seen as decreasing BRET ratio. Figure created with BioRender.com.

A BRET setup consists of two essential parts, a donor and an acceptor, in the case of TRUPATH which is the RLuc8 (donor) and GFP2 (acceptor). There are several different BRET methods, that all have varying donors, acceptors, and substrates. TRUPATH uses BRET2.

To initiate the BRET a substrate that makes RLuc8 bioluminescence/emit light is added. For BRET2 this is Coelenterazine 400a (Deep Blue C™). When the GFP2 is near the RLuc8 it will start to fluoresce, and the light intensity for both RLuc8 and GFP2 is measured at their respective emission wavelength, that is around 395 nm for RLuc8 and 510 nm for GFP2. *(Note, when we performed a spectral scan of our setup it showed that the peak for RLuc8 emission was at 420 nm, and therefore*

decided to measure at 420 nm instead of 395 nm. This information is further acknowledged in the discussion section of this thesis). This means that when the RLuc8 and GFP2 are close, in the case of TRUPATH and GPCR signalling is when the heterotrimer is associated we will measure a high signal from both RLuc8 and GFP2, and then, as the ligand is added, a decrease in signal is measured since the heterotrimer dissociates, and GFP2 is no longer close enough to RLuc8 to be able to fluoresce.

The overall measurement is thus, a measurement of loss of BRET signal which correlates to GPCR signalling. There are two common ways of presenting BRET data. The first one being BRET ratio, where the raw counts of emission intensity at 510 nm (GFP2) is divided by the raw counts of emission intensity at 395 nm (RLuc8). The other one is netBRET, where the BRET ratio values are subtracted by the mean value of the blank/lowest concentration of substrate BRET ratio values, to get a curve that starts at zero.

Materials and Methods

TRUPATH-kit
The TRUPATH kit was obtained from Addgene (addgene.org) (ref. Kit #1000000163). The kit contains plasmids encoding each of the α-, β-, and γ-subunits that are stated in supplementary information in Table A. The plasmids are sent in bacteria (ampicillin-resistant) as agar stab. The bacterial agar stab is cultured in ampicillin enriched LB-medium (Substratafdelingen-Panum) and stored as glycerol stocks (50:50 glycerol to bacteria) at -80 °C.

Plasmid purification of TRUPATH constructs
A pipette tip dipped in the frozen bacterial-glycerol stock containing the different TRUPATH plasmids is transferred to a shake flask, 300 mL of LB-medium (Substratafdelingen-Panum) and 0.33 mL of ampicillin (Sigma-Aldrich ref. A5354-10ML) is added and incubated in a shake incubator (at 37 °C, 180 rpm) overnight. The suspension is transferred to centrifuge bottles and centrifuged at 6000xg for 10 minutes. The media is removed from the pellet. The purification column NucleoBond® Xtra Midi kit (Macherey-Nagel) is then used to isolate the DNA according to the manufacturer's protocol.

DNA sequencing
The TRUPATH constructs were sequenced by Eurofins Genomics. A declaration of the primers used for each construct is presented in supplementary information in Table B. Pairwise sequence alignment with the known DNA sequence (obtained from addgene.org – TRUPATH Kit ##1000000163) for respective construct was performed in Geneious Prime.

Cell culture
HEK293 WT cells (ATCC) were maintained and passaged in T175 flasks in Gibco™ DMEM (1X) + GlutaMAX™ -I 1966 media with added 10 % FBS (Substratafdelingen-Panum) and 1 % Pen-Strep (Substratafdelingen-Panum) and incubated at 37 °C and 5 % CO_2 overnight.

Single-cell suspension preparation
The cell media in the cultivation flask is removed by suction. Cells are washed with 10 mL PBS (Substratafdelingen-Panum). 2 mL Trypsin EDTA (Lonza - cat: BE17-161E) is added and left to incubate for 2-5 min. 10 mL cell media (Gibco™ DMEM (1X) + GlutaMAX™ -I 1966) is added

to stop the trypsinization, media is pipetted up and down to ensure proper mixing and then transferred to a falcon tube. 10 µL of solution 13 AO•DAPI (ChemoMetec A/S ref. 910-3013) is added to 190 µL of the cell suspension in an Eppendorf tube and mixed well. 10 µL of the mix is added to a glass slider (NC-Slide A8) and put into the NucleoCounter NC-3000 (Chemometec), cell viability and density.

About the method: Trypsin is added to facilitate cell detachment from the culture flask in which the cells are cultured. Solution 13 contains two different dyes, AO which stains all nucleated cells and DAPI that stains all non-viable cells, this is so it is possible to count the amount of live as well as dead cells in the suspension.

Cell seeding (96 well plate)

White 96-well microplates (Culture Plate™) are coated with 60 µL poly-D-lysine (Sigma-Aldrich ref. P7886) suspended in PBS (Substratafdelingen-Panum) and incubated at RT for 30 minutes. Right before addition of the single-cell suspension the poly-D-lysine is removed, and plate is washed with 100 µL PBS (Substratafdelingen-Panum) per well.

The single-cell suspension is diluted with cell media Gibco™ DMEM (1X) + GlutaMAX™ -I 1966 for HEK293 WT and Gibco™ DMEM (1X) + GlutaMAX™ -I 1885 for COS7, to obtain 20.000 cells (COS7 cells) or 35.000 (WT HEK293 cells) per well. 100 µL is added to each well. The cells are left to incubate at 37 °C and 5 % CO_2 ON.

About the method: Poly-D-lysine is used to coat the 96-well plates to mimic a synthetic extracellular matrix thus enhancing the cell adhesion to the plate.

Transfection with lipofectamine, HEK293 WT cells

For each white 96-well microplate (Culture Plate™), all cell media is removed and 50 µL Gibco™ Opti-MEM is added to each well. The DNA to be transfected (TRUPATH biosensor – obtained from Addgene and receptor to be investigated (declaration of receptors is presented in supplementary information in Table C)) is added into Opti-MEM (amount of Opti-MEM is decided by No. of wells to be transfected, 25 µL/well) and mixed by vortex. The rest of the Opti-MEM (25 µL per well) is mixed with lipofectamine (Invitrogen ref. 11668-09) (3 µL/well) and left to incubate for 5 minutes at RT. The DNA solution and lipofectamine solution is mixed and incubated for 20 minutes at RT. 50 µL of the DNA-lipofectamine solution is added to the wells and left to incubate for 5 h, at 37 °C and 5 % CO_2.

After 5 h, the DNA-lipofectamine solution is removed and replaced with fresh media (Gibco™ DMEM (1X) + GlutaMAX™ -I 1966), 100 µL/well and is left to incubate at 37 °C and 5 % CO_2 overnight.

About the method: This transfection method utilizes lipofection, where the DNA to be delivered to the cells are entrapped in a liposome and can thus pass over the cell membrane.

Transfection with calcium phosphate precipitation, COS7 cells
For each plate (96-well) to be transfected, 380 µL Tris EDTA-buffer (Substratafdelingen-Panum), 60 µL $CaCl_2$ (Lab technician associated with CMBR 6th floor) and DNA is mixed and slowly dropped into 480 µL 2x HBS (Hepes Buffered Saline – Substratafdelingen-Panum) during slow vortex. The mixture is incubated for 45 min at RT.

300 µL Chloroquine (Sigma, C6628-25G) is added to 10 mL of cell media (Gibco™ DMEM (1X) + GlutaMAX™ -I 1885), the DNA mixture is added to the cell media and mixed gently. The old cell media from the plate to be transfected is removed and 100 µL of the new cell media + DNA mixture is added to each well. The plate is incubated for 5 h at 37 °C.

After 5 h, the media is removed and replaced with fresh media (100 µL/well) and is left to incubate at 37 °C and 5 % CO_2 overnight.

TRUPATH – BRET2
Cells were transfected for one day[1], for a declaration of the TRUPATH construct combinations used when transfecting see supplementary information in Table D. The plate is washed with 100 µL HBSS (1X) (Gibco ref. 14025-050) per well. 85 µL HBSS is added to each well. 10 µL of 50 µM Coelenterazine 400a (NanoLight Technology Cat. # 340-500) (dissolved in absolute EtOH) is added to each well. The plate is incubated for 5 minutes at 37 °C. 5 µL of the ligand (declaration of ligands/agonists used is presented in supplementary information in Table C) is added to each well and the plate is read with 410/80 and 515/30 emission filters by the CLARIOstar® Plus (BMG Labtech) for 5 cycles (0, 2, 4, 6 and 8 minutes).

Treatment of HEK293 WT cells with PTX
After transfection with lipofectamine, cell media (Gibco™ DMEM (1X) + GlutaMAX™ -I 1966) containing 100 ng/mL of PTX (Sigma – CAT nr. P2980) is added to the wells and left to incubate at 37 °C ON.

About the method: Pertussis toxin, PTX is an ADP-ribosylation enzyme that targets the αi subunit blocking it from coupling with GPCRs, and thus inhibiting all Gi-signalling.

Sequence alignments
Sequences for all G proteins as well as for mGPR91 and hGPR91 were collected from UniProt. For a declaration of the sequences used see supplementary information in Table E. ICM Molsoft was used to perform pairwise as well as multiple sequence alignments. To decide what part of each G protein sequence that interacted with the GPCR we used crystal structures where a GPCR had been crystallized together with a bound α-subunit. For the Gi-family we used the PDB structure 6LFO and for the Gq-family 7DFL as references.

[1] In the published article regarding TRUPATH (Olsen et al., 2020), transfection was performed for two days. Since we used a slightly different transfection method, we did a comparison of 1- versus 2-day transfection, results from this can be found in Figure 7.

Results

Optimization of the TRUPATH biosensor platform

Since TRUPATH has not been used in the research group earlier, the first phase of this thesis was to implement TRUPATH and optimize it to the preferred transfection- and seeding method used in the lab, and the specific plate reader used.

Sequencing of TRUPATH constructs

To ensure that the 14 different TRUPATH constructs obtained from addgene had the correct sequence that they stated with the kit, and that we had successfully purified them, we started by sequencing them. No deviations were observed for any of the constructs. Data not shown.

1-day versus 2-day transfection

Olsen et al. (2020), used a two-day transfection method where the transfections first were made in 6-well dishes for one day, then re-seeded in 96-well plates for another day before conducting the assay. The common protocol in our lab for transfection of HEK-cells is to seed the cells and then transfect them directly in the 96-well plates, just having a 1-day transfection period. So, to evaluate if there was any significant difference between transfecting for 1- versus 2-days we made one transfection mixture that was then left to transfect the cells for either one or two days. The results are presented in Figure 7. The curves for 1-day and 2-day transfection are presented with netBRET values to clearly see if the same BRET-window/efficacy was obtained. The curves have similar looks and the same endpoint, meaning they produce the same window.

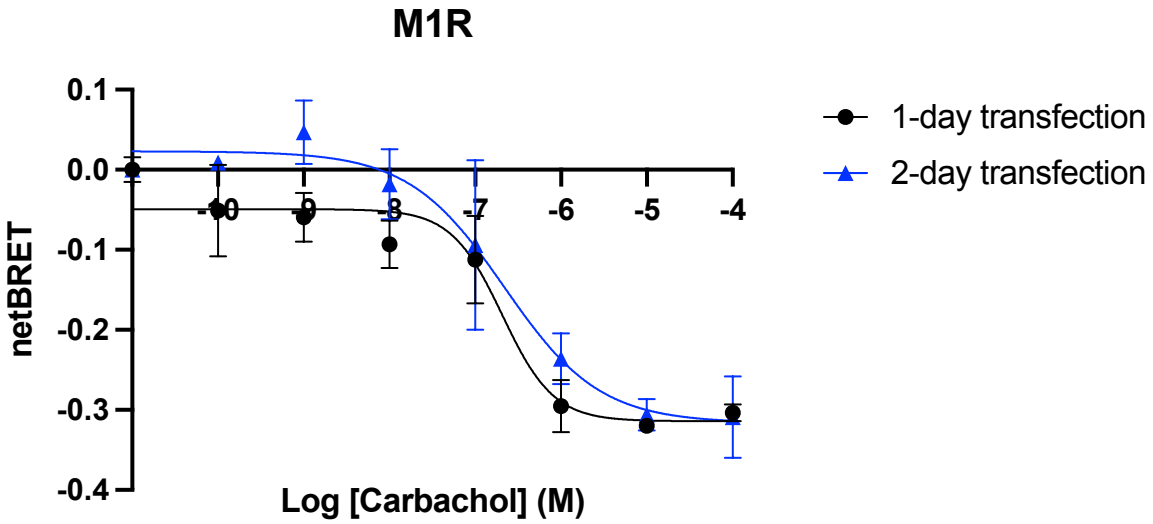

Figure 7. netBRET 510 nm/ 395 nm against x-axis of log(carbachol) (M), for 1- versus 2-day transfection. 1-day transfection presented as black dots, data shows mean value from triplicates ± SD, first time-point measured, 0 min. 2-day transfection presented by blue triangles, data shows mean value form duplicate ± SD, first time-point measured, 0 min. TRUPATH constructs used: αQ – β3 – γ9.

The receptor used for this part of the optimization was Muscarinic acetylcholine receptor 1 (M1R). The reason for using this receptor was because it is a known strong Gq-coupled receptor.

Transfection-ratio of receptor to TRUPATH constructs

M1R and D2R

Olsen et al. (2020) stated a use of a 1:1 ratio with regards to the receptor and TRUPATH constructs when transfecting the HEK 293 WT cells. To evaluate if this was the best ratio, we investigated how the response changed when changing the amount of receptor, both M1R and Dopamine receptor 2 (D2R), and the amount of TRUPATH constructs respectively. We used M1R and D2R because they are known to couple strongly to Gq and Gi respectively. Thus, we could evaluate the actual assay without it being disturbed by poor coupling of the receptor. The results are presented in Figure 8, A and B shows BRETratio and netBRET respectively for Gq-coupled M1R. In A, the starting point is more or less the same for all ratios except for 1:5 (pink triangles) which starts a bit higher in signal indicating that more of the TRUPATH constructs will result in a higher starting value. In B, showing the netBRET values of M1R the biggest window is obtained by 1:1 (red squares). Figure 8 C and D shows BRETratio and netBRET respectively for the Gi-coupled D2R. In C all curves look pretty much the same indicating no direct difference, the "outlier" is the ratio of 5:1 (blue circles) that has a significantly lower starting value than the rest of the curves and also a smaller window (as seen in D) and does not follow the same sigmoidal shape as the rest of the curves. The curves for Gi-coupled D2R (Figure 8, C) have a starting point that is about double the one of the Gq-coupled M1R (Figure 8, A), also the overall window is approximately 1 log bigger for D2R (Gi) than M1R (Gq) (Figure 8 B and D).

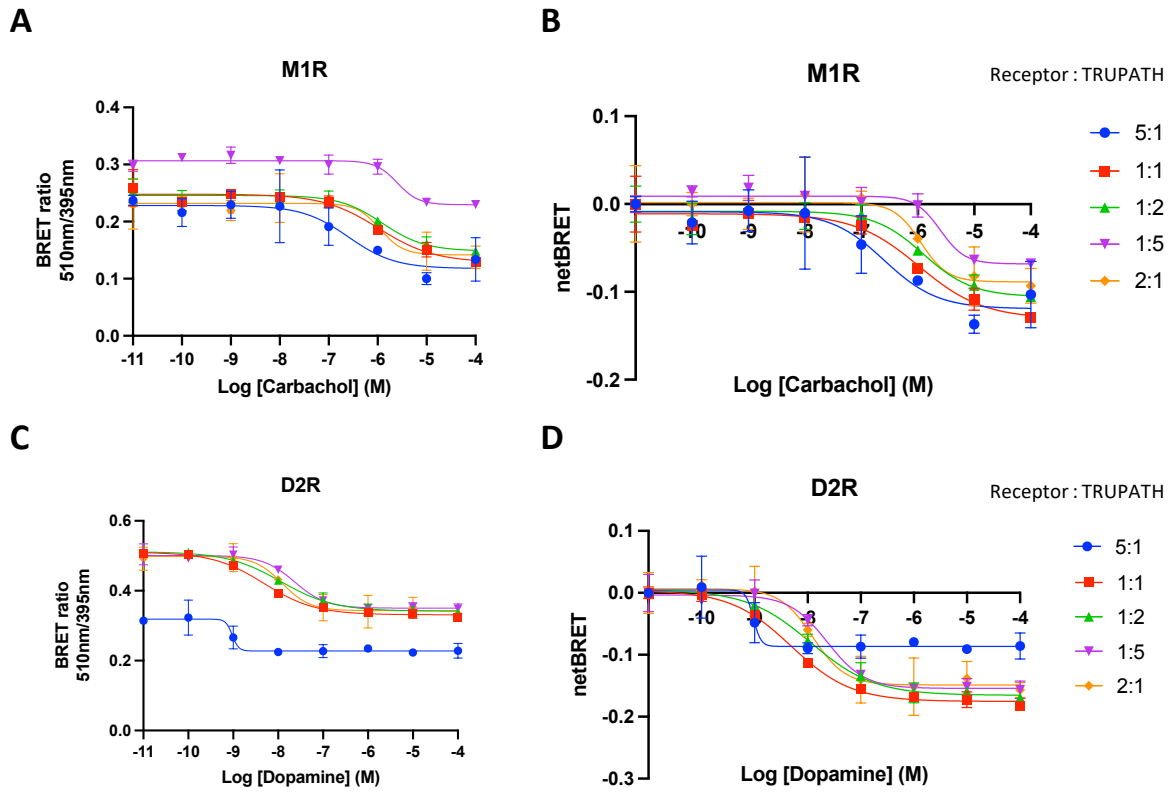

Figure 8. Comparison of different transfection ratios between receptor and TRUPATH constructs. Ratios presented as receptor:TRUPATH constructs. Men value of duplicates ± SD, obtained from the first measuring point at 0 min. A and B. BRETratio (510 nm/395 nm) and netBRET against x-axis of log (Carbachol) (M) for M1R – Gαq coupled. C and D. BRETratio (510 nm/395 nm) and netBRET against x-axis of log (Dopamine) (M) for D2R – Gαi2 coupled.

GPR91 – Gi constructs

When the research group have been doing previous transfections with GPR91, 20 ng of construct is normally used since it is usually not expressed as strongly as for example M1R and D2R. To see if this was the best amount to use together with the TRUPATH constructs we transfected with varying amounts (5 ng – 10 ng – 20 ng – 40 ng) of hGPR91 and mGPR91 and constant amount of TRUPATH constructs (5 ng) and measured the BRETratio. Results are shown in Figure 9. In parallel with these trials, we also performed spectral scans (see next section) because of the results obtained from the spectral scans, the BRETratio measurements were performed at 510 nm and 420 nm instead of the previous 510 nm and 395 nm.

For hGPR91 both 20 ng (ratio 4:1, green) and 40 ng (ratio 8:1, pink) gave good responses, meaning that they have the same starting point as well as the same window and overall curve-shape (Figure 9 - A), for mGPR91 5 ng (ratio 1:1, blue), 10 ng (ratio 2:1, red) and 20 ng (ratio 4:1, green) were more or less identical and 40 ng (ratio 8:1, pink) a bit worse as the shape of the curve does not follow the wanted sigmoidal shape (Figure 9 – B). Worth noticing is that this part of the optimization was only done for GPR91 together with Gi. Later, further optimization attempts for GPR91 together with Gq was performed.

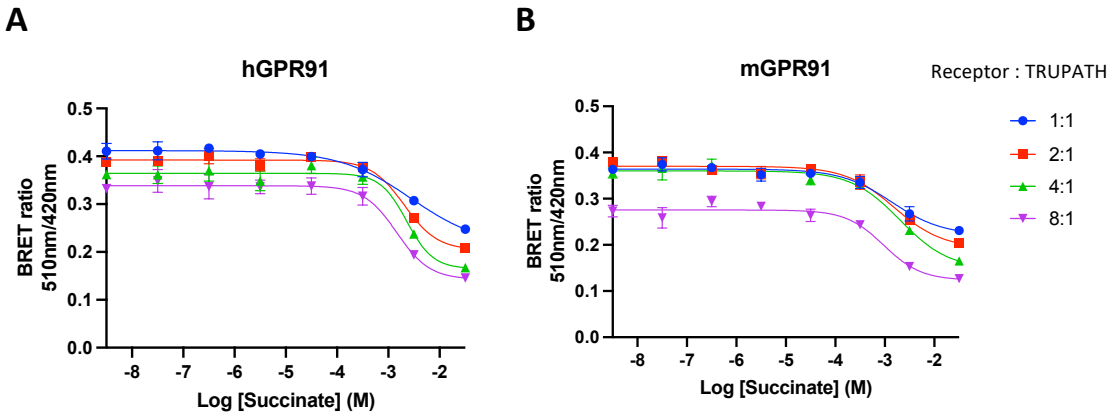

Figure 9. BRETratio (510 nm/420 nm) for different ratios of receptor to constant TUPATH constructs against Log (Succinate) (M). Ratio presented as receptor:TRUPATH constructs. Mean value of triplicates ± SD, obtained from first measuring point at 0 min. A. results for hGPR91 coupled to Gαi2. B. Results for mGPR91 coupled to Gαi2.

Spectral scans – optimal measuring wavelengths and ratio of TRUPATH constructs

After the transfection optimization we wanted to see if it was possible to obtain a more efficacious response. The hypothesis behind this optimization step was that since the plate reader used did not have emission filters for the specific wavelengths in BRET2, 395 nm and 510 nm, the measurement can be considered an approximation of the light emitted at the chosen wavelengths. Also, since BRET2 is known for its considerably lower emission intensity compared to BRET1, measuring the emitted light without filers could be a challenge. So, therefore we tried changing the ratio between α and βγ, 1:1:1, 1:2:2 and 1:3:3 (α:β:γ), aiming at getting an overall higher response and thus get more reliable results. Results are presented in Figure 10.

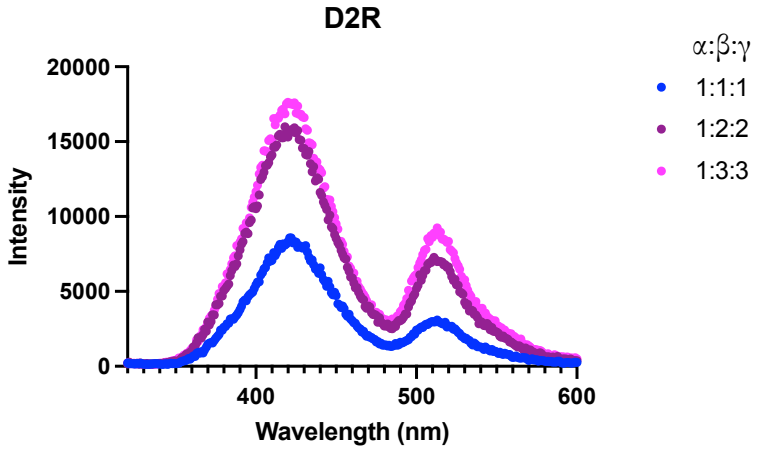

Figure 10. Ratio presented as α:β:γ. Emission intensity for every wavelength. Measurements performed at unstimulated D2R (Gi). One measurement was taken for every wavelength.

The spectral scans show emission intensity on the y-axis and each wavelength on the x-axis making it possible to clearly identify the emission peaks as well as if there is an increase in emitted light. As can be seen in Figure 10, there is a significant increase when changing the ratio of the TRUPATH constructs, where the ratio of 1:3:3 is the one that produces the highest intensity of emitted light.

Note! *All BRET data presented until here in the optimization part of the results are measured without emission filters. Further on, emission filters were obtained since it was considered that it was needed to be able to produce more sensitive results.*

GPR91 - Gq optimization

When proceeding to work with GPR91 and analysing its recruitment and coupling to the Gq-family we encountered some issues when using the same optimized method as for GPR91 together with the Gi – family. The curves obtained were not consistent and some Gq-family members did not work at all. Since previous studies done within the group have shown Gq-recruitment with functional assays we determined to see if we could optimize the method further to be able to work consistently together with the Gq-family also. This optimization part was performed with GPR91 as well as with Human neurotensin receptor 1 (hNTSR1), which is a known strong Gq-recruiting receptor.

Amount of receptor

First, we wanted to see if a change in the amount of receptor transfected could improve the GPR91 coupling to Gq, see Figure 11 for a comparison of 5, 10, 20 and 40 ng of hGPR91 transfected in HEK293 WT cells together with 5:5:15 (α:β:γ) ng of αQ-constructs. 10, 20 and 40 ng all give good sigmoidal-shaped curves. 5 ng have a lower starting point as well as no curve. There is an observed difference in starting point between 10 ng and 20 ng, and 40 ng. The reason for the different starting points of the different amounts of receptors is not known. In some of the previous runs we would observe that more of the receptor would lead to a decrease in starting point whilst here we observe the opposite.

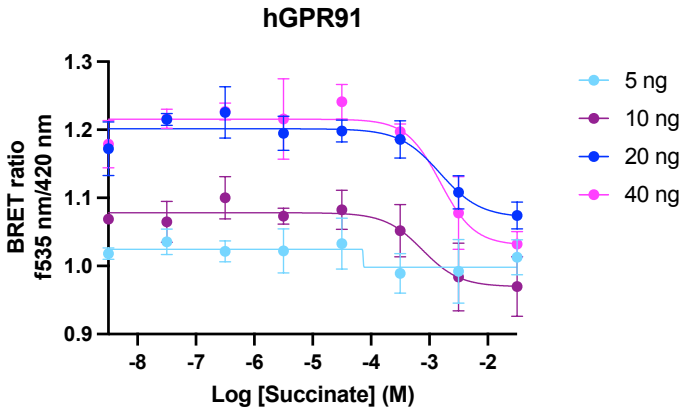

Figure 11. BRET ratio (f535/420 nm), comparison of different amounts of hGPR91 together with αQ. Data is mean value of triplicates ± SD. Timepoint 4 min.

Inhibition of endogenous Gi-family proteins

HEK 293 WT cells endogenously express all G protein families. To see if it might be endogenous Gi proteins that were disturbing the GPR91's ability to couple stably with Gq we treated the cells with pertussis toxin (PTX), a potent Gi-inhibitor. Results are presented in Figure 12, recruitment of Gq for hGPR91 was not improved by the cells PTX treatment, instead it resulted in a worse curve-shape and less efficacy. hNTSR1 was not affected by the PTX treatment at all. Results for 5, 10 and 40 ng of hGPR91 is not shown since it was determined to proceed with 20 ng of GPR91.

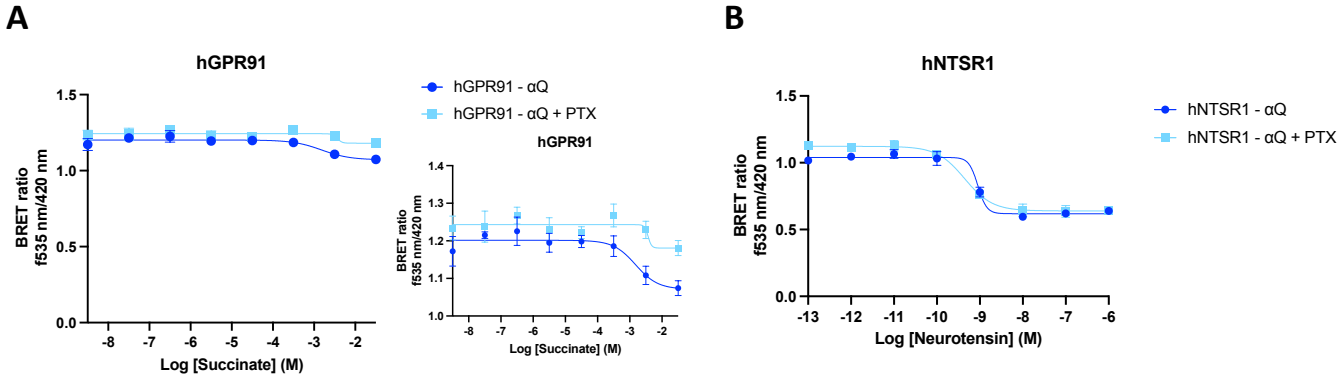

Figure 12. BRET ratio, comparison of (A) hGPR91 (20 ng) together with αQ, with and without treatment with PTX. (B) hNTSR1 together with αQ with and without treatment with PTX. Data is mean value from triplicates ± SD. Timepoint 4 min.

Run-time and ligand incubation

We also tried to add the agonist at the same time as coelenterazine 400a, letting the cells incubate for 5 minutes with succinate present to see if it would make any difference in response. This had no significant effect on getting bigger windows and more consistent curves. Data not shown. We also ran the experiment for 18 minutes instead to see if we might get better curves after longer run time. This also did nothing to improve our results. Data not shown.

COS-7 cells

A last attempt to get more consistent results was made by using the same method as for the Gi-family but in a different cell line, COS7-cells. This did also not improve any of the parameters that we value, efficacy/window size, and sigmoidal curve profiles. Data not shown.

mGPR91 and hGPR91 – Gi *vs.* Gq

Presented in Figure 14 are the activation/recruitment of the different alpha subunits of the Gi-family and the Gq-family for both human and murine GPR91. The data is presented as netBRET that have been normalized against D2R for Gi and hNTSR1 for Gq. The reason for doing this is to minimize the inevitable variations between the different runs when working with cells and transfection. Also since some data is run with one emission filter and some data is run with two emission filters. Both D2R and hNTSR1 have produced consistent curves with little standard error of the mean (SEM) between the different runs, see supplementary information in Figure A, making it a representable way to present the data. As seen in the figure, with an exception for mGPR91 together with αQ there is clear recruitment of all the G proteins in both the Gi-family (αi1, αi2, αi3, αoA, αoB and αz) and the Gq-family (αQ, α11, and α15). Another general trend that is observed is that mGPR91 is more potent than hGPR91, but they have the same efficacy (except for αi3 where mGPR91 is more efficacious than hGPR91 and the opposite for α11 where hGPR91 seems to be more efficacious). The empty vector generated no response, except in αi2 where a little response is seen, this is not thought to be relevant or affect the results. For the Gi-family (A-F) the highest efficacy is with αi2, and the lowest for αz, and the rest being similar in efficacy. The Gq-family (G-I) shows similar efficacy for αQ and α11 (for human) and an apparently much greater efficacy for α15.

Figure 13 presents the logarithmic EC50 value for each of the different alpha subunits in the Gi- and the Gq-family for both hGPR91 (pink) and mGPR91 (blue). The EC50 value is half the concentration needed to obtain full receptor activation. Thus, it gives us an indication of the potency of each of the receptors together with each α-subunit. The EC50 values are obtained from the graphs in Figure 14 making this another way of presenting the data. As mentioned before, murine is consistently more potent than human, except for αQ, where no recruitment with mGPR91 was observed. Looking at the respective receptor, mGPR91 (blue bars) it appears to recruit αi2 the best followed by α11 and αoB whilst for hGPR91 (pink bars) α11 has the most potent EC50 value followed by α15 and αi2. For additional information and data regarding the EC50 values, see supplementary information in Figure B-C and Table F.

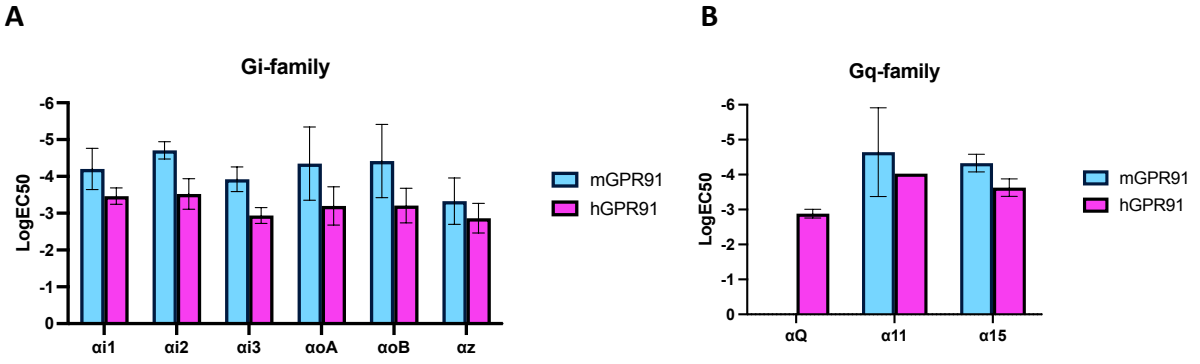

Figure 13. EC50 value of each alpha-subunit within the Gi- and the Gq-family together with hGPR91 and mGPR91. Data shown as mean values ± SD. No. of N and timepoints are presented in supplementary information in Table F. This shows that mGPR91 is consistently more potent than hGPR91. Data not shown for mGPR91 together with αQ since no curves were obtained indicating that there is no or weak recruitment.

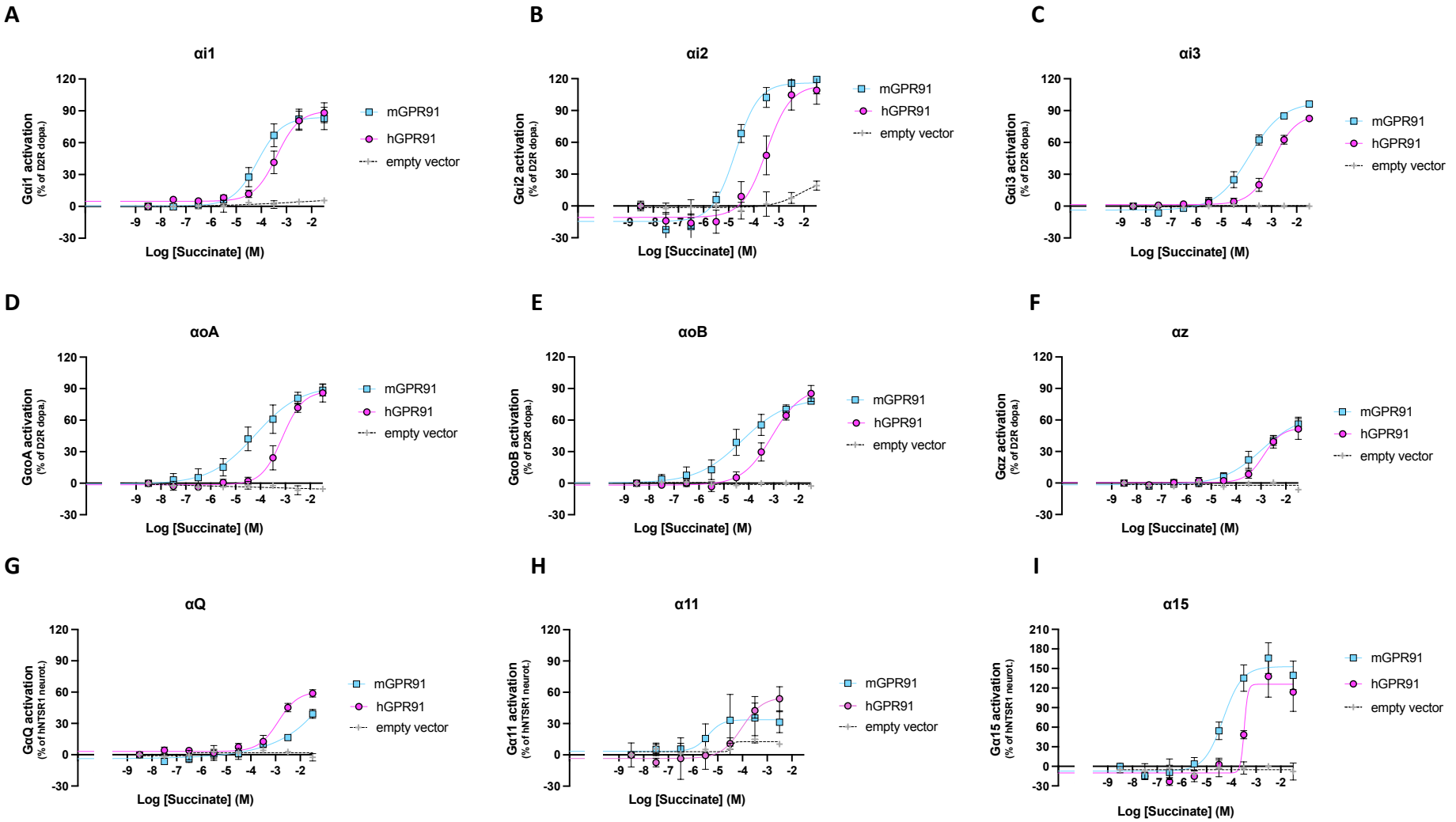

Figure 14. Graphs presenting the recruitment/signalling of each of the different α-subunits in the Gi- and the Gq-family together with mGPR91 and hGPR91 as well as an empty vector run for each as a percentage of D2R activation with dopamine for the Gi-family and hNTSR1 activation with neurotensin for the Gq-family. The plots of the empty vectors are the mean value from triplicate values (N=1) ± SD. The plots for αi1, αi2, αi3, αoA, αoB, and αz **(A-F)** are mean values of N=4, each N consisting of triplicates ± SEM. αQ **(G)** is mean values of N=3 each N consisting of triplicates, ± SEM. α11 **(H)** is mean values of N=1 for hGPR91 triplicates ± SD and N=2 for mGPR91, each N consisting of triplicates, ± SEM. α15 **(I)** is mean values of N=3, each run consisting of triplicates, ± SEM. Timepoints for the different runs are presented in supplementary information Table F.

To be able to evaluate the results further we also made sequence alignments of the α-subunit of all G proteins (Figure 15) as well as between the human and murine receptor (Figure 16). Amino acid colours in alignments represent consensus strength from strongest: dark green, light green, light yellow, and white. As presented in the background the GPCR interacts mainly with the C-termini and amino acids close to the C-termini of the G protein. Therefore, the part of the sequence that is presented in the Figure 15, is only this part of the G protein, the full alignment is presented in supplementary information in Figure D. In both the Gi- and Gq-family there are parts with low consensus that could be a factor affecting the different potencies within the families. Comparing just αi1, αi2, and αi3, they have very high similarity, 91 %, the same goes for αoA and αoB that have a similarity of 86 % and especially for αQ and α11 which have 100 % similarity. Comparing the subunits of both the Gi-family and the Gq-family they have low similarity, 43 % and several parts with low consensus.

A

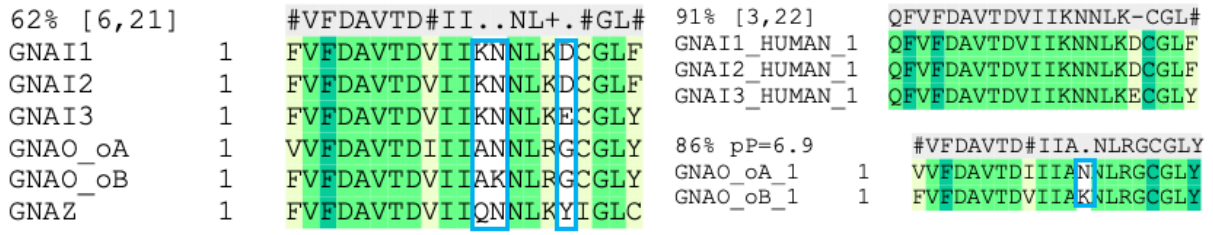

B

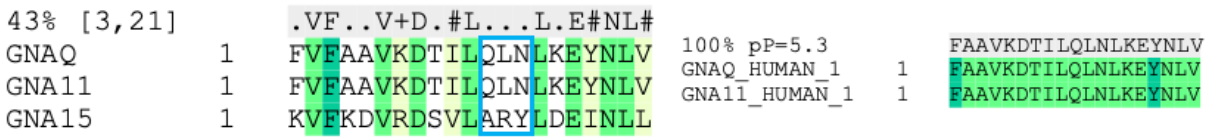

C

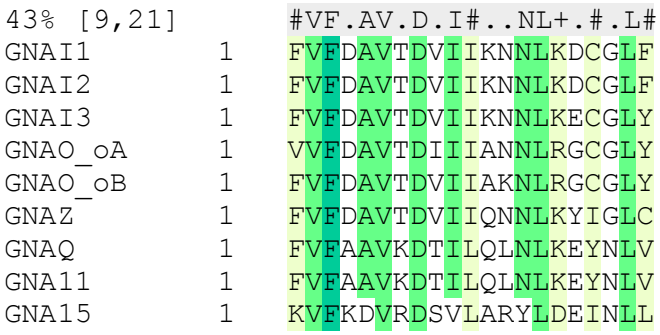

Figure 15. Alignments of the main part of a G protein α-subunit that interacts with a GPCR. A) α-subunits of the Gi-family B) α-subunits of the Gq-family C) α-subunits of both Gi- and Gq-family. Amino acid colours in alignments represent consensus strength from strongest: dark green (conserved between all G-proteins), light green, light yellow, and white. Blue squares highlight regions of low consensus (A and B). Percentage represents sequence similarity.

As presented in Figure 16, where the red squares highlight structurally important parts of GPR91 when it comes to interaction with the α-subunit of G proteins, and the blue squares highlight parts with low consensus within the red squares. We observe that there are several parts of the sequences with low consensus that could explain the difference in potency between hGPR91 and mGPR91.

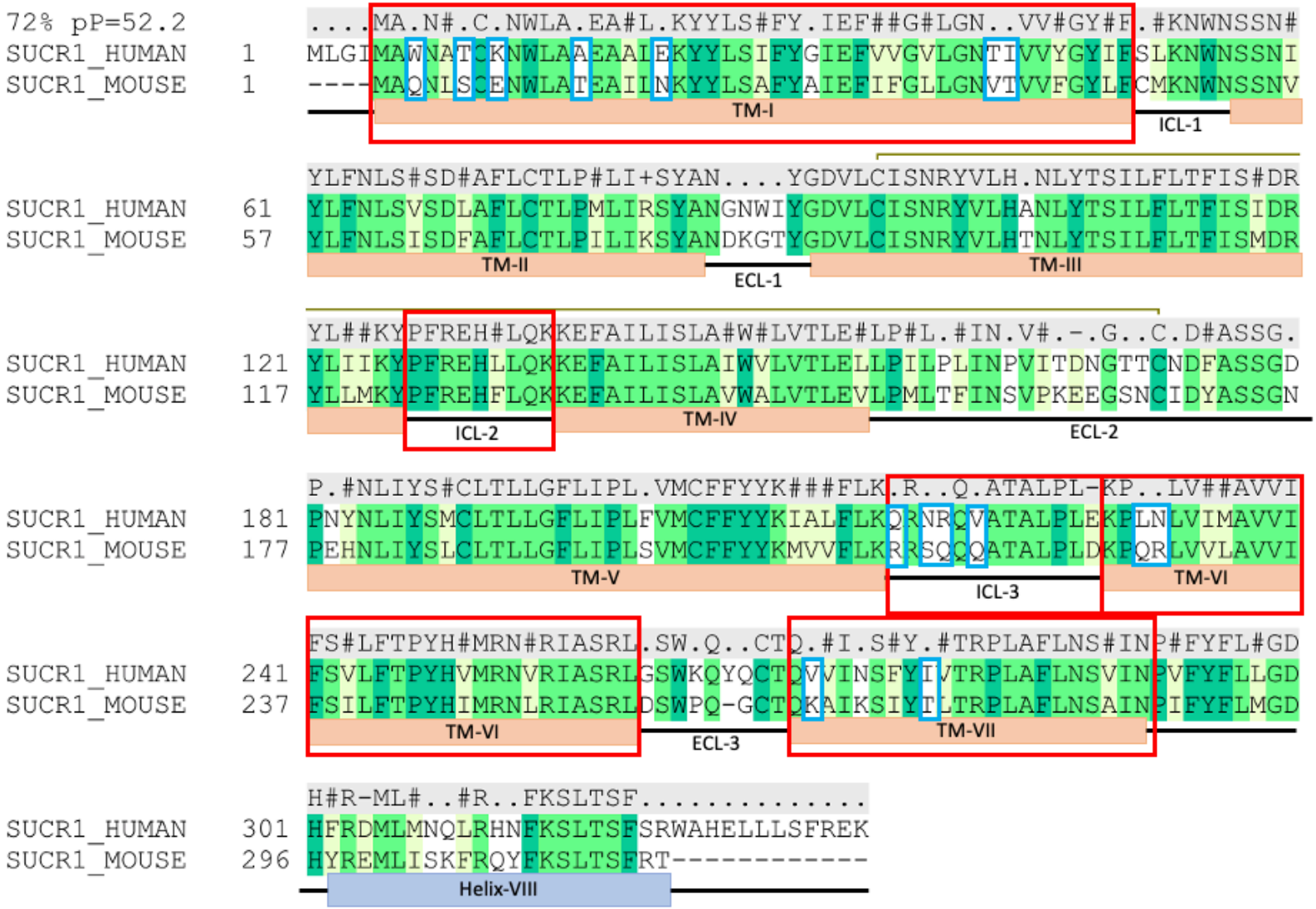

Figure 16. Pairwise sequence alignment of hGPR91 (top) and mGPR91 (bottom). Red squares show parts of GPR91 that interacts with the α-subunit of the G protein. Blue squares are amino acids without consensus within the red squares between the two sequences. Colour of amino acids correlated to consensus strength from strong to none, dark green (conserved residues within the class A GPCRs), light green, light yellow, and white.

Discussion

Optimization of the TRUPATH biosensor platform

Below follows one discussion section for each result section presented above.

1-day versus 2-day transfection

As seen in Figure 7*,* the results for the 1-day versus 2-day transfection showed no significant difference, they both produced a good sigmoidal curve which had equally big windows. Since we could not detect any clear advantage of doing a 2-day transfection, it was determined to continue with 1-day transfection for HEK-293 WT cells. This was mainly due to the short length of this project, so we were able to work as efficiently as possible. However, sometimes in the lab it has been observed that some receptor targets prefer a 2-day transfection in HEK293 WT cells over a 1-day transfection period. Thus, it is suggested to compare when starting to work with a new receptor.

Transfection-ratio of receptor to TRUPATH constructs

M1R and D2R

The transfection-ratio of receptor to TRUPATH constructs were tested on both M1R and D2R as these are known to couple and signal strongly via Gq and Gi respectively (Bonci & Hopf, 2005; Maeda et al., 2019). Since we are expecting GPR91 to signal via both Gi and Gq we wanted to make sure that the optimization was done for both G proteins in order to achieve optimal results in both families. The results showed that the stated ratio of 1:1 (Figure 8 B and D) was indeed the one that resulted in the best overall curves and the biggest window/best efficacy when considering both M1R (Gq) and D2R (Gi). The two "outlier curves" 1:5 ratio for M1R and 5:1 ratio for D2R suggests that too much of the TRUPATH constructs can affect the overall signal output by for example clustering together just by the shear amounts of constructs which will result in a higher starting value and not as big window due to dissociation since there are not enough receptors to recruit them all. The 5:1 ratio for D2R however indicates that too much receptor would lead to a lower starting signal and smaller BRET-window, this could be due to constitutive activity, but cannot be concluded for certain. With regards to constitutive receptor activity (when the receptor spontaneously isomerizes to its active state and thus signals without any ligand), it can be observed in the figure showing BRETratio (Figure 8) where the starting point for all ratios are more or less the same, leading us to conclude that there should not be any issue with constitutive activity as long as not more than 20 ng of receptor is transfected in. Having constitutive activity, we would expect to be seeing a lower starting point in the graphs showing the BRETratio (Figure 8 A and C) as we add more of the receptor. As for M1R in the red-curve, orange-curve and blue curve, we increase the amount of receptor added but held the amount of TRUPATH the same, in which no direct effect of constitutive activity is observed. For D2R however, when transfecting 40 ng, a slightly lower starting point is obtained leading us to believe that it could be because of constitutive receptor activity. Although, the only way to evaluate constitutive activity is by using an inverse agonist, which unfortunately is not available on the market for GPR91.

GPR91 – Gi constructs

Since we did not observe a significant difference between transfecting 40 ng (8:1) and 20 ng (4:1) for hGPR91, and for mGPR91 20 ng was a bit better with regards to starting point and overall efficacy, it was determined to transfect with 20 ng of GPR91, ratio 4:1 to not put more stress than necessary on the cell. We could also observe the same phenomena as with the previous D2R when transfecting in 40 ng of receptor, as a lower starting value was observed that could be an indication of constitutive activity, but as mentioned previously, without an inverse agonist this cannot be concluded. Also, since we have observed varying starting points for each run, and not being able to explain what affects these observations one could run an empty vector control together with each run to conclude the effect of expressing the receptor on the TRUPATH constructs.

Spectral scans – optimal measuring wavelengths and ratio of TRUPATH constructs

An interesting observation made when performing the spectral scans was that the emission peak for RLuc8, which is stated to be at 395 nm (Olsen et al., 2020) was according to our spectral scan instead at 420 nm. This resulted in the BRET-measurements made after this discovery being instead performed at 510 nm and 420 nm. The resellers of the substrate used, Coelenterazine 400a (NanolightTechnology™) state that the emission peak for the RLuc8 is around 400 nm. Looking at other studies performed (Dacres et al., 2012, 2013; De et al., 2009) we can only conclude that the emission maxima of RLuc8 seem to vary from group to group and what kind of machine is used, and that is probably beneficial to first do a spectral scan with the machine used to measure the assay to see what emission maxima you have.

However, since we changed the detection wavelength when we made the discovery it should not have affected our results. The data that was produced when measuring at 395 nm could be affected in the way that the actual BRET data is not directly comparable to the ones measured at 420 nm since we might expect lower intensity and thus a lower count of the RLuc8 emission when measuring outside of its peak. However, the trends that we have seen is not affected and the conclusions drawn in the early optimization can still be regarded as reliable. Also worth noticing is that the big advantage of using BRET2 over other BRET-assays is that the two emission peaks are far apart on the spectrum and thus do not spill over to each other making it highly specific.

The results showed that with an increased ratio of β and γ in relation to α, higher overall response was indeed obtained (Figure 10). This was expected since more of the β- and γ-units present in the cell would increase the possibility of coupling to the α-unit and then signalling further, which is what we are measuring in the BRET-assay. Looking at Figure 10, 1:2:2 (purple circles) and 1:3:3 (magenta circles) the first peak at 420 nm is almost at the same intensity, however at the 510 nm peak there is an observable difference in intensity between the two, in the favour of 1:3:3, therefore this was concluded to be the best ratio within the TRUPATH constructs.

Moving further along, we however decided to continue with the ratio 1:1:3 (α:β:γ). The decision to do this was based on firstly, that the GFP2 is attached to the γ-subunit, and to get a higher response from the GFP2 it is only the γ-subunit that should affect that. Secondly, transfecting the cells with a lot of DNA can be very stressful, and can lead to them not expressing everything as consistently as possible. Therefore, we decided to ease up the stress on the cells by decreasing the amount of

β-constructs again. Although, after obtaining emission filters for BRET2, we tried transfecting with 1:1:1 (data not shown) and it showed as good results as with the 1:1:3 ratio. However, the filters were obtained quite late in the project, so to be able to have all runs comparable we decided to stick with the 1:1:3, even after we started using the emission filters.

GPR91 Gq optimization

Amount of receptor

As the previous receptor titration together with the Gi-family, now with the Gq-family, both 20 ng and 40 ng of receptor showed the best results, as presented in Figure 11. We determined to move forward as previous with 20 ng of GPR91 to firstly stress the cells as little as possible and secondly to obtain as coherent protocol as possible. An observation that differs from previous experiments is that for hGPR91 with Gq we get a higher starting point the more receptor we transfect, the opposite was observed for D2R, mGPR91 and hGPR91 together with Gi, where more receptor resulted in a lower starting point. The reason for this phenomenon is not known.

Inhibition of endogenous Gi-family proteins

Throughout the project we have had difficulties obtaining consistent results with GPR91 together with the Gq-family whilst the control-receptor hNTSR1 worked great with all the Gq-family. To combat this problem, the next step was to see if HEK-293 WT endogenous Gi-family proteins were disturbing the GPR91's possibility to couple and signal via Gq. Since we assume that GPR91's coupling to Gq is weak and that it prefers Gi coupling we treated the cells with PTX, a potent Gi-family inhibitor (Katada, 2012). Presented in Figure 12: A, hGPR91 showed no improvement, but rather worse signalling in the cells treated with PTX and for hNTSR1, Figure 12: B, there is no significant difference between the two conditions even though hNRST1 have been documented to also signal via Gi (Besserer-Offroy et al., 2017b). Thus, we can confidently conclude that the observed response is indeed Gq signalling. This further led us to conclude that the poor signalling obtained from the Gq-family together with GPR91 was not due to endogenous Gi-family proteins in the HEK293 WT cells but rather poor coupling between the receptor (GPR91) and the Gq-family.

Run-time and ligand incubation

With the background knowledge of that GPR91 couples more poorly to the Gq-family than the Gi-family we wanted to see if we could get better signalling via the Gq-family if we gave the cells longer time to acclimatize to the GPR91 and Gq-family constructs together with succinate, thus increasing the probability of having Gq recruitment. Usually binding of an agonist happens within nanoseconds of its encountering with the receptor leading this hypothesis to be a long shot. And as it turned out and is also stated in the result section, we could not observe any difference between with and without ligand incubation nor between the response obtained in the beginning of the run versus the ones in the end.

Concluding remarks regarding GPR91 - Gq optimization

As we were unable to improve the results obtained, we decided to continue with the protocol as optimized with the Gi-family. This also means that the poorer results presented of the Gq in comparison to Gi can be attributed to the weak coupling of GPR91 to Gq and not to the assay

itself. Presented in supplementary information in Figure A is the data for D2R and hNTSR1. Comparing the results we obtained with other studies, the EC50 value for D2R with dopamine varies a bit depending on what kind of assay you use. Dai and colleagues presented an EC50 value of 0.56 nM using and Ca^{2+} mobilization assay (Dai et al., 2018), Free and colleagues performed both a Ca^{2+} accumulation assay and a cAMP inhibition assay and presented EC50 values of 2.5 nM and 60 nM for respective assay (Free et al., 2014), lastly Sung and colleagues presented an EC50 value of 9.7 nM using a membrane potential assay (Sung et al., 2016). The ranges of these presented EC50 values are in line with what we obtained. The same goes for hNTSR1, where Besserer-Offroy and colleagues presents an EC50 value of 1.84 nM for hNTSR1 with neurotensin using a similar BRET assay as us (Besserer-Offroy et al., 2017), it is a little bit higher but still in the same range, also they use CHO-KI cells and we use HEK293 WT, a factor that could affect the overall result.

The fact that our obtained EC50 values are in line with others indicates that the TRUPATH assay can be used as an accurate biosensor for strong GPCRs. Trauelsen and colleagues have previously shown Gq recruitment in hGPR91 using a different BRET based assay (Trauelsen et al., 2021), so it could be that the TRUPATH assay might not sensitive enough to pick up weak coupling events.

mGPR91 and hGPR91 – Gi *vs.* Gq

Recruitment

As has been shown in different functional assays in previous studies (He et al., 2004; Trauelsen et al., 2021) we show that GPR91 recruit both Gi- and Gq-family G proteins. hGPR91 is shown to recruit all G protein alpha subunits investigated and mGPR91 all but αQ.

Looking at the strength of recruitment between Gi and Gq, it is clear that GPR91 recruits Gi more consistently and stronger than Gq. All Gi runs made resulted in clear curves and the SEM between the four runs that are presented in Figure 14 are small, concluding that the results for the Gi-family are reliable and comparable. The Gq recruitment was not as stable as can be seen in the number of successful runs that make up the curves presented (Figure 14), the deviations between the runs are also bigger for the Gq-family than for the Gi-family. Due to the instability of the Gq-recruitment results they could be argued to not be as comparable when looking at the Log EC50 values, however, the Gq-family in its entirety is recruited by GPR91, which is what we wanted to substantiate in this thesis.

The Gi-family

Presented in Figure 14 A-F are the G proteins of the Gi-family. The fact that GPR91 recruits Gi in general is well known (He et al., 2004). However, this information is obtained by various functional assays where a selected downstream mediator is measured. For Gi it is often measurement of cAMP inhibition. These functional assays do not discriminate between α-subunits within the Gi-family and therefore we wanted to see if there are any differences in how the GPR91 is recruiting and if it can relate to where the different G proteins are expressed as well as where we know that GPR91 is expressed and have a functional role. We see that GPR91 clearly and consistently recruits all the Gi-family. αi2 showed the highest efficacy and it is expressed in adipose tissue, where GPR91 is also highly expressed. We could speculate a correlation between these results.

However, when aligning the GPCR-binding part of αi1, αi2, and αi3, they show 91 % similarity and only two amino acids that have low consensus, which suggest that they should interact with GPR91 very similarly. Looking to the EC50 values, αi2 is the one with the lowest value (lowest concentration needed for receptor activation) for both human and murine GPR91, indicating that GPR91 preferred Gi-family member is αi2. Looking at the two isomers in the Gi-family, αoA and αoB, they have the same EC50 value as well as efficacy for both human and murine. This is expected since they have 86 % sequence similarity at the part that interacts with GPCRs and only one amino acid where there is no consensus. αz has the highest EC50 value, and lowest efficacy it also has the least sequence similarity to the rest of the Gi-family which could potentially be an explanation to the observed results.

The Gq-family

All data available for GPR91 coupling to either Gi or Gq are obtained from various functional assays. When looking at Gq-signalling one often measures either Ca^{2+} accumulation or mobilization or IP accumulation. Ca^{2+} signalling, normally thought of as Gq signalling, can however also be activated by the βγ-dimer, which makes it harder to fully attribute the Ca^{2+} accumulation or mobilization to Gq-signalling directly. The biggest breakthrough regarding GPR91 and signalling via Gq came from Trauelsen and colleagues that showed that hyperpolarization of human M2 macrophages was mediated through Gq-signalling (Trauelsen et al., 2021). We observed that hGPR91 indeed recruit αQ, α11, and α15 of the Gq-family whilst mGPR91 only recruits α11 and α15. So, hGPR91 recruited both αQ and α11 with similar efficacy but with approximately 1 Log lower for α11 than αQ suggesting that hGPR91 prefers α11 over αQ. However, since the data for α11 with human is only based on one successful run, this is not stated to be 100 % exact regarding the exact EC50 value, but instead just shows that the recruitment is happening.

α15

The odd-one-out when looking to efficacy, not just in its own family but over both the families are α15. α15 appears to be much more efficacious than all other G proteins, this result should however be looked at with some caution. α15 is well known to be a promiscuous G protein (Offermanns & Simon, 1995), meaning it has the ability to interact with a wide range of GPCRs. Hauser et. al. (2022) also show that the Gq-family of G proteins is the second largest with regards to the No. of GPCRs they are known to recruit, and within the Gq-family α15 recruits the most unique GPCRs (Hauser et al., 2022). Another thing worth noticing is that since the data is normalized against hNTSR1 receptor we assume that hNTSR1 recruits all of the Gq-family members equally good, which we do not know for certainty, and thus it seems like GPR91 is extremely efficacious in recruiting α15.

Human vs. murine

Comparing the human GPR91 and murine GPR91, the murine GPR91 is consistently around ½ log to 1 log more potent than human GPR91. This is a phenomenon that has been observed previously (Rexen Ulven et al., 2018; Trauelsen et al., 2017b). Thus, murine is more sensitive and recruits G proteins at lower succinate concentrations. The reason for this is not known and is a great aspect of future research. Looking at the sequence alignment, there are differences between the two species in residues that interact with the G protein.

Conclusions

Optimization

The assay TRUPATH was successfully optimized and implemented with some deviations from the original protocol published by Olsen et al., (2020). We used a 1-day transfection method and changed the ratio between the TRUPATH constructs to 1:1:3 (α:β:γ). We also showed that the ratio between receptor and TRUPATH constructs was fine to use 1:1 (receptor:TRUPATH) when working with a strongly expressed receptor, whilst when working with a less strong receptor this could need to be altered to obtain satisfactory results. Therefore, it is suggested to perform a receptor titration to see what ratio/amount of receptor produces the best results. Also, we observed the emission maxima for RLuc8 to be at 420 nm and not 395 nm which was stated by Olsen et al., (2020) leading us to recommend doing a spectral scan as described in the results to determine the exact wavelength for the machine to be used.

GPR91

As has been shown in previous functional assays GPR91 recruits both the Gi- and the Gq-family, it recruits the Gi-family more consistently than Gq. We show a full characterization of the recruitment profile of human and murine GPR91 looking at potency and efficacy for the Gi- and Gq-family of G proteins. There seems to be structural differences between the human and murine GPR91 that affects the receptors potency, where murine is consistently more potent than human.

Future research aspects and improvements

The TRUPATH biosensor

The TRUPATH biosensor has shown big potential with investigation GPCRs recruitment profile and can be a great tool to more precisely characterize GPCRs. A potential use could be to use TRUPATH to further develop the GPCR databank (gpcrdb.org) to involve exact G protein coupling charts within each G protein family. Since GPCRs are targets for many drugs, the more knowledge we have about how they work, the better drugs can be developed.

Constitutive activity

The initial hypothesis we made was that a lower starting value of the BRETratio was an indication of constitutive activity. However, this was not consistent throughout our experiments leading us to be unable to make any claims with regards to if GPR91 is constitutive or not. To test this, we would need to use an inverse agonist. The inverse agonist binds the same binding site as the agonist and blocks spontaneous signalling. It also favours the "resting" state of the receptor and thus lowering the overall signalling mediated through the receptor population. As of now there is no inverse agonist on the market for GPR91.

MD-simulations

This thesis gave us a good initial thought about key aspects of how GPR91 couples and that there is a clear difference between human and murine receptors. Moving further along it is suggested to perform simulations where comparison of human and murine is one focus, Gi versus Gq is another focus, as well as investigating the binding event of succinate to GPR91 and how that affects the

two different focuses mentioned. The goal with the simulations is to identify key amino acids involved, and then take that into the lab to perform mutations and see what effects can be observed. All resulting in getting a better knowledge about GPR91 with regards to G protein binding.

A further aspect that could be subject for improvement with regards to performing good simulations is the lack of a crystal structure for both human and murine GPR91. The only available crystal structure of GPR91 today is of rat GPR91 bound to antagonist. For the subsequent simulations we will use homology models of mGPR91 and hGPR91. An available crystal structures of the investigated receptor will result in more precise simulations.

Ligand bias

In this thesis we have only shown that succinate via GPR91 can recruit both Gi and Gq, an interesting thing to look more into is if it is affected by for example ligand bias. Since GPR91 is known to be able to signal by activation of for example other TCA-cycle intermediates, that are all present naturally in human cells it would be interesting to see if other ligands would show different results compared to the endogenous ligand succinate. Trauelsen and colleagues have shown that there are some synthetic compounds that are Gi biased with GPR91 (Trauelsen et al., 2021).

References

Besserer-Offroy, É., Brouillette, R. L., Lavenus, S., Froehlich, U., Brumwell, A., Murza, A., Longpré, J. M., Marsault, É., Grandbois, M., Sarret, P., & Leduc, R. (2017a). The signaling signature of the neurotensin type 1 receptor with endogenous ligands. *European Journal of Pharmacology*, *805*, 1–13. https://doi.org/10.1016/J.EJPHAR.2017.03.046

Besserer-Offroy, É., Brouillette, R. L., Lavenus, S., Froehlich, U., Brumwell, A., Murza, A., Longpré, J.-M., Marsault, É., Grandbois, M., Sarret, P., & Leduc, R. (2017b). The signaling signature of the neurotensin type 1 receptor with endogenous ligands. *European Journal of Pharmacology*, *805*, 1–13. https://doi.org/10.1016/j.ejphar.2017.03.046

Bonci, A., & Hopf, F. W. (2005). The Dopamine D2 Receptor: New Surprises from an Old Friend. *Neuron*, *47*(3), 335–338. https://doi.org/10.1016/j.neuron.2005.07.015

Chemtob, S., Ste-Justine, R. C.-C., Hamel, D., Sanchez, M., Duhamel, F., Roy, O., Honoré, J.-C., Noueihed, B., Zhou, T., Nadeau-Vallée, M., Hou, X., Lavoie, J.-C., Mitchell, G., & Mamer, O. A. (2013). *G-Protein-Coupled Receptor 91 and Succinate Are Key Contributors in Neonatal Postcerebral Hypoxia-Ischemia Recovery*. https://doi.org/10.1161/ATVBAHA.113.302131

Chouchani, E. T., Pell, V. R., Gaude, E., Aksentijević, D., Sundier, S. Y., Robb, E. L., Logan, A., Nadtochiy, S. M., Ord, E. N. J., Smith, A. C., Eyassu, F., Shirley, R., Hu, C. H., Dare, A. J., James, A. M., Rogatti, S., Hartley, R. C., Eaton, S., Costa, A. S. H., … Murphy, M. P. (2014). Ischaemic accumulation of succinate controls reperfusion injury through mitochondrial ROS. *Nature*, *515*(7527), 431–435. https://doi.org/10.1038/NATURE13909

Correa, P. R. A. V., Kruglov, E. A., Thompson, M., Leite, M. F., Dranoff, J. A., & Nathanson, M. H. (2007). Succinate is a paracrine signal for liver damage. *Journal of Hepatology*, *47*(2), 262–269. https://doi.org/10.1016/J.JHEP.2007.03.016

Dacres, H., Michie, M., Anderson, A., & Trowell, S. C. (2013). Advantages of substituting bioluminescence for fluorescence in a resonance energy transfer-based periplasmic binding protein biosensor. *Biosensors and Bioelectronics*, *41*(1), 459–464. https://doi.org/10.1016/J.BIOS.2012.09.004

Dacres, H., Michie, M., Wang, J., Pfleger, K. D. G., & Trowell, S. C. (2012). Effect of enhanced Renilla luciferase and fluorescent protein variants on the Förster distance of Bioluminescence resonance energy transfer (BRET). *Biochemical and Biophysical Research Communications*, *425*(3), 625–629. https://doi.org/10.1016/J.BBRC.2012.07.133

Dai, W.-L., Liu, X.-T., Bao, Y.-N., Yan, B., Jiang, N., Yu, B.-Y., & Liu, J.-H. (2018). Selective blockade of spinal D2DR by levo-corydalmine attenuates morphine tolerance via suppressing PI3K/Akt-MAPK signaling in a MOR-dependent manner. *Experimental & Molecular Medicine*, *50*(11), 1–12. https://doi.org/10.1038/s12276-018-0175-1

De, A., Ray, P., Loening, A. M., & Gambhir, S. S. (2009). BRET3: a red-shifted bioluminescence resonance energy transfer (BRET)-based integrated platform for imaging protein-protein interactions from single live cells and living animals. *The FASEB Journal*, *23*(8), 2702–2709. https://doi.org/10.1096/fj.08-118919

de Castro Fonseca, M., Aguiar, C. J., Antônio, J., Franco, R., Gingold, R. N., & Leite, M. F. (2016). *GPR91: expanding the frontiers of Krebs cycle intermediates*. https://doi.org/10.1186/s12964-016-0126-1

de Francesco, E., Sotgia, F., Clarke, R., Lisanti, M., & Maggiolini, M. (2017). G Protein-Coupled Receptors at the Crossroad between Physiologic and Pathologic Angiogenesis: Old Paradigms and Emerging Concepts. *International Journal of Molecular Sciences*, *18*, 2713. https://doi.org/10.3390/ijms18122713

Fernández-Veledo, S., Ceperuelo-Mallafré, V., & Vendrell, J. (2021). Rethinking succinate: an unexpected hormone-like metabolite in energy homeostasis. *Trends in Endocrinology & Metabolism*, *32*(9), 680–692. https://doi.org/10.1016/j.tem.2021.06.003

Fredriksson, R., Lagerström, M. C., Lundin, L.-G., & Schiöth, H. B. (2003). The G-Protein-Coupled Receptors in the Human Genome Form Five Main Families. Phylogenetic Analysis, Paralogon Groups, and Fingerprints. *Molecular Pharmacology*, *63*(6), 1256. https://doi.org/10.1124/mol.63.6.1256

Free, R. B., Chun, L. S., Moritz, A. E., Miller, B. N., Doyle, T. B., Conroy, J. L., Padron, A., Meade, J. A., Xiao, J., Hu, X., Dulcey, A. E., Han, Y., Duan, L., Titus, S., Bryant-Genevier, M., Barnaeva, E., Ferrer, M., Javitch, J. A., Beuming, T., … Sibley, D. R. (2014). Discovery and Characterization of a G Protein–Biased Agonist That Inhibits β -Arrestin Recruitment to the D2 Dopamine Receptor. *Molecular Pharmacology*, *86*(1), 96–105. https://doi.org/10.1124/mol.113.090563

Gilissen, J., Jouret, F., Pirotte, B., & Hanson, J. (2016). Insight into SUCNR1 (GPR91) structure and function. *Pharmacology & Therapeutics*, *159*, 56–65. https://doi.org/10.1016/J.PHARMTHERA.2016.01.008

Gurevich, V. v, & Gurevich, E. v. (2019). GPCR Signaling Regulation: The Role of GRKs and Arrestins. *Frontiers in Pharmacology*, *10*. https://doi.org/10.3389/fphar.2019.00125

Hakak, Y., Lehmann-Bruinsma, K., Phillips, S., Le, T., Liaw, C., Connolly, D. T., & Behan, D. P. (2009). The role of the GPR91 ligand succinate in hematopoiesis. *Journal of Leukocyte Biology*, *85*(5), 837–843. https://doi.org/10.1189/jlb.1008618

Hauser, A. S., Avet, C., Normand, C., Mancini, A., Inoue, A., Bouvier, M., & Gloriam, D. E. (2022). Common coupling map advances GPCR-G protein selectivity. *ELife*, *11*. https://doi.org/10.7554/eLife.74107

Hauser, A. S., Chavali, S., Masuho, I., Jahn, L. J., Martemyanov, K. A., Gloriam, D. E., & Babu, M. M. (2018). Pharmacogenomics of GPCR Drug Targets. *Cell*, *172*(1–2), 41-54.e19. https://doi.org/10.1016/j.cell.2017.11.033

He, W., Miao, F. J.-P., Lin, D. C.-H., Schwandner, R. T., Wang, Z., Gao, J., Chen, J.-L., Tian, H., & Ling, L. (2004). Citric acid cycle intermediates as ligands for orphan G-protein-coupled receptors. *Nature*, *429*(6988), 188–193. https://doi.org/10.1038/nature02488

Hilger, D., Masureel, M., & Kobilka, B. K. (2018). Structure and dynamics of GPCR signaling complexes. *Nature Structural & Molecular Biology*, *25*(1), 4–12. https://doi.org/10.1038/s41594-017-0011-7

Katada, T. (2012). The Inhibitory G Protein Gi Identified as Pertussis Toxin-Catalyzed ADP-Ribosylation. *Biological and Pharmaceutical Bulletin*, *35*(12), 2103–2111. https://doi.org/10.1248/bpb.b212024

Latorraca, N. R., Venkatakrishnan, A. J., & Dror, R. O. (2017). GPCR Dynamics: Structures in Motion. *Chemical Reviews*, *117*(1), 139–155. https://doi.org/10.1021/acs.chemrev.6b00177

Liu, K., Wu, L., Yuan, S., Wu, M., Xu, Y., Sun, Q., Li, S., Zhao, S., Hua, T., & Liu, Z.-J. (2020). Structural basis of CXC chemokine receptor 2 activation and signalling. *Nature*, *585*, 135. https://doi.org/10.1038/s41586-020-2492-5

Macaulay, I. C., Tijssen, M. R., Thijssen-Timmer, D. C., Gusnanto, A., Steward, M., Burns, P., Langford, C. F., Ellis, P. D., Dudbridge, F., Zwaginga, J.-J., Watkins, N. A., van der Schoot, C. E., & Ouwehand, W. H. (2006). Comparative gene expression profiling of in vitro differentiated megakaryocytes and erythroblasts identifies novel activatory and inhibitory platelet membrane proteins. *Blood*, *109*(8), 3260–3269. https://doi.org/10.1182/blood-2006-07-036269

Maeda, S., Qu, Q., Robertson, M. J., Skiniotis, G., & Kobilka, B. K. (2019). Structures of the M1 and M2 muscarinic acetylcholine receptor/G-protein complexes. *Science*, *364*(6440), 552–557. https://doi.org/10.1126/science.aaw5188

Martínez-Reyes, I., & Chandel, N. S. (2020). Mitochondrial TCA cycle metabolites control physiology and disease. *Nature Communications*, *11*(1), 102. https://doi.org/10.1038/s41467-019-13668-3

Mills, E. L., Harmon, C., Jedrychowski, M. P., Xiao, H., Garrity, R., Tran, N. v., Bradshaw, G. A., Fu, A., Szpyt, J., Reddy, A., Prendeville, H., Danial, N. N., Gygi, S. P., Lynch, L., & Chouchani, E. T. (2021). UCP1 governs liver extracellular succinate and inflammatory pathogenesis. *Nature Metabolism*, *3*(5), 604–617. https://doi.org/10.1038/s42255-021-00389-5

Neves, S. R., Ram, P. T., & Iyengar, R. (2002). G Protein Pathways. *Science*, *296*(5573), 1636–1639. https://doi.org/10.1126/science.1071550

Offermanns, S., & Simon, M. I. (1995). Gα15 and Gα16 Couple a Wide Variety of Receptors to Phospholipase C. *Journal of Biological Chemistry*, *270*(25), 15175–15180. https://doi.org/10.1074/jbc.270.25.15175

Olsen, R. H. J., DiBerto, J. F., English, J. G., Glaudin, A. M., Krumm, B. E., Slocum, S. T., Che, T., Gavin, A. C., McCorvy, J. D., Roth, B. L., & Strachan, R. T. (2020). TRUPATH, an open-source biosensor platform for interrogating the GPCR transducerome. *Nature Chemical Biology*, *16*(8), 841–849. https://doi.org/10.1038/s41589-020-0535-8

Palczewski, K., Kumasaka, T., Hori, T., Behnke, C. A., Motoshima, H., Fox, B. A., Trong, I. le, Teller, D. C., Okada, T., Stenkamp, R. E., Yamamoto, M., & Miyano, M. (2000). Crystal Structure of Rhodopsin: A G Protein-Coupled Receptor. *Science*, *289*(5480), 739–745. https://doi.org/10.1126/science.289.5480.739

Regard, J. B., Sato, I. T., & Coughlin, S. R. (2008). Anatomical Profiling of G Protein-Coupled Receptor Expression. *Cell*, *135*(3), 561–571. https://doi.org/https://doi.org/10.1016/j.cell.2008.08.040

Rexen Ulven, E., Trauelsen, M., Brvar, M., Lückmann, M., Bielefeldt, L. Ø., Jensen, L. K. I., Schwartz, T. W., & Frimurer, T. M. (2018). Structure-Activity Investigations and Optimisations of Non-metabolite Agonists for the Succinate Receptor 1. *Scientific Reports*, *8*(1), 10010. https://doi.org/10.1038/s41598-018-28263-7

Ristic, B., Bhutia, Y. D., & Ganapathy, V. (2017). Cell-surface G-protein-coupled receptors for tumor-associated metabolites: A direct link to mitochondrial dysfunction in cancer. *Biochimica et Biophysica Acta (BBA) - Reviews on Cancer*, *1868*(1), 246–257. https://doi.org/10.1016/J.BBCAN.2017.05.003

Rosenbaum, D. M., Rasmussen, S. G. F., & Kobilka, B. K. (2009). The structure and function of G-protein-coupled receptors. *Nature*, *459*(7245), 356–363. https://doi.org/10.1038/nature08144

Rubic, T., Lametschwandtner, G., Jost, S., Hinteregger, S., Kund, J., Carballido-Perrig, N., Schwärzler, C., Junt, T., Voshol, H., Meingassner, J. G., Mao, X., Werner, G., Rot, A., & Carballido, J. M. (2008). Triggering the succinate receptor GPR91 on dendritic cells enhances immunity. *Nature Immunology*, *9*(11), 1261–1269. https://doi.org/10.1038/ni.1657

Sapieha, P., Sirinyan, M., Hamel, D., Zaniolo, K., Joyal, J. S., Cho, J. H., Honoré, J. C., Kermorvant-Duchemin, E., Varma, D. R., Tremblay, S., Leduc, M., Rihakova, L., Hardy, P., Klein, W. H., Mu, X., Mamer, O., Lachapelle, P., di Polo, A., Beauséjour, C., … Chemtob, S. (2008). The succinate receptor GPR91 in neurons has a major role in retinal angiogenesis. *Nature Medicine*, *14*(10), 1067–1076. https://doi.org/10.1038/NM.1873

Schiöth, H. B., & Fredriksson, R. (2005). The GRAFS classification system of G-protein coupled receptors in comparative perspective. *General and Comparative Endocrinology*, *142*(1–2), 94–101. https://doi.org/10.1016/J.YGCEN.2004.12.018

Smith, J. S., Lefkowitz, R. J., & Rajagopal, S. (2018). Biased signalling: from simple switches to allosteric microprocessors. *Nature Reviews Drug Discovery*, *17*(4), 243–260. https://doi.org/10.1038/nrd.2017.229

Sriram, K., & Insel, P. A. (2018). G Protein-Coupled Receptors as Targets for Approved Drugs: How Many Targets and How Many Drugs? *Molecular Pharmacology*, *93*(4), 251. https://doi.org/10.1124/mol.117.111062

Sung, Y.-M., Wilkins, A. D., Rodriguez, G. J., Wensel, T. G., & Lichtarge, O. (2016). Intramolecular allosteric communication in dopamine D2 receptor revealed by evolutionary amino acid covariation. *Proceedings of the National Academy of Sciences*, *113*(13), 3539–3544. https://doi.org/10.1073/pnas.1516579113

Trauelsen, M., Hiron, T. K., Lin, D., Petersen, J. E., Breton, B., Husted, A. S., Hjorth, S. A., Inoue, A., Frimurer, T. M., Bouvier, M., O'Callaghan, C. A., & Schwartz, T. W. (2021). Extracellular succinate hyperpolarizes M2 macrophages through SUCNR1/GPR91-mediated Gq signaling. *Cell Reports*, *35*(11), 109246. https://doi.org/10.1016/j.celrep.2021.109246

Trauelsen, M., Rexen Ulven, E., Hjorth, S. A., Brvar, M., Monaco, C., Frimurer, T. M., & Schwartz, T. W. (2017a). Receptor structure-based discovery of non-metabolite agonists for the succinate receptor GPR91. *Molecular Metabolism*, *6*(12), 1585–1596. https://doi.org/10.1016/J.MOLMET.2017.09.005

Trauelsen, M., Rexen Ulven, E., Hjorth, S. A., Brvar, M., Monaco, C., Frimurer, T. M., & Schwartz, T. W. (2017b). Receptor structure-based discovery of non-metabolite agonists for the succinate receptor GPR91. *Molecular Metabolism*, *6*(12), 1585–1596. https://doi.org/10.1016/J.MOLMET.2017.09.005

Vargas, S. L., Toma, I., Kang, J. J., Meer, E. J., & Peti-Peterdi, J. (2009). Activation of the Succinate Receptor GPR91 in Macula Densa Cells Causes Renin Release. *Journal of the American Society of Nephrology*, *20*(5), 1002. https://doi.org/10.1681/ASN.2008070740

Worzfeld, T., Wettschureck, N., & Offermanns, S. (2008). G12/G13-mediated signalling in mammalian physiology and disease. *Trends in Pharmacological Sciences*, *29*(11), 582–589. https://doi.org/10.1016/j.tips.2008.08.002

Wu, J. Y., Huang, T. W., Hsieh, Y. T., Wang, Y. F., Yen, C. C., Lee, G. L., Yeh, C. C., Peng, Y. J., Kuo, Y. Y., Wen, H. T., Lin, H. C., Hsiao, C. W., Wu, K. K., Kung, H. J., Hsu, Y. J., & Kuo, C. C. (2020). Cancer-Derived Succinate Promotes Macrophage Polarization and Cancer Metastasis via Succinate Receptor. *Molecular Cell*, *77*(2), 213-227.e5. https://doi.org/10.1016/J.MOLCEL.2019.10.023

Xia, R., Wang, N., Xu, Z., Lu, Y., Song, J., Zhang, A., Guo, C., & He, Y. (2021). Cryo-EM structure of the human histamine H1 receptor/Gq complex. *Nature Communications*, *12*(1), 2086. https://doi.org/10.1038/s41467-021-22427-2

Zhang, D., Zhao, Q., & Wu, B. (2015). Structural Studies of G Protein-Coupled Receptors. *Molecules and Cells*, *38*(10), 836–842. https://doi.org/10.14348/molcells.2015.0263

Supplementary information

Abbreviation list

Abbreviation	Definition
AC	Adenylyl cyclase
ACE	Angiotensin converting enzyme
BRET	Bioluminescence Resonance Energy Transfer
cAMP	Cyclic adenosine monophosphate
CES	cis-epoxy succinic acid
COX-2	Cyclooxygenase-2
DAG	Diacyl glycerol
ddNTP	Dideoxynucleotides triphosphates
ER	Endoplasmic reticulum
ETC	Electron transport chain
FDA	US Food and Drug Administration
GPCRs	G protein-coupled receptors
GRKs	G protein-coupled receptor kinases
GPR91	G protein-coupled receptor 91 (same as SUCNR1)
HSC	Hepatic stellate cells
IP_3	Inositol trisphosphate
JGA	Juxtaglomerular apparatus
MAPKs	Mitogen-activated protein kinases
PDB	Protein Data Bank
PKA	Protein kinase A
PKC	Protein kinase C
PLC	Phospholipase C
PIP_2	Phosphatidylinositol 4,5-bisphosphate
PTX	Pertussis toxin
RAS	Renin-angiotensin system
SUCNR1	Succinate receptor 1 (same as GPR91)
TCA-cycle	Tricarboxylic acid cycle
VEGF	Vascular endothelial growth factor

Materials and Methods

Contents of TRUPATH-kit

Table A. List of contents in TRUPATH-kit (addgene.org ref. kit #1000000163). G protein subunit and its corresponding full vector name.

G protein subunit	Full vector name
alpha-subunits	
αi1	pcDNA5/FRT/TO-GAlphai1-RLuc8
αi2	pcDNA5/FRT/TO-GAlphai2-RLuc8
αi3	pcDNA5/FRT/TO-GAlphai3-RLuc8
αoA	pcDNA5/FRT/TO-GAlphaoA-RLuc8
αoB	pcDNA5/FRT/TO-GAlphaioB-RLuc8
αz	pcDNA5/FRT/TO-GAlphaz-RLuc8
αGust.	pcDNA5/FRT/TO-GAlphaGustducin-RLuc8
αsS	pcDNA5/FRT/TO-GAlphasS-RLuc8
αsL	pcDNA5/FRT/TO-GAlphasL-RLuc8
αQ	pcDNA5/FRT/TO-GAlphaQ-RLuc8
α11	pcDNA5/FRT/TO-GAlpha11-RLuc8
α15	pcDNA5/FRT/TO-GAlpha15-RLuc8
α12	pcDNA5/FRT/TO-GAlpha12-RLuc8
α13	pcDNA5/FRT/TO-GAlpha13-RLuc8
beta-subunits	
β1	pcDNA3.1-Beta1
β3	pcDNA3.1-Beta3
gamma-subunits	
γ1	pcDNA3.1-GGamma1-GFP2
γ8	pcDNA3.1-GGamma8-GFP2
γ9	pcDNA3.1-GGamma9-GFP2
γ13	pcDNA3.1-GGamma13-GFP2

Primers for sequencing

Table B. Primers used for sequencing for each TRUPATH construct.

Addgene reference	Construct	Primer name	Forward primer 5' – 3'	Primer name	Reverse primer 5' – 3'
A1	αi1	CMV	CGCAAATGGGCGGTAGGCGTG	bGH	TAGAAGGCACAGTCGAGG
A2	αi2	CMV	CGCAAATGGGCGGTAGGCGTG	bGH	TAGAAGGCACAGTCGAGG
A3	αi3	CMV	CGCAAATGGGCGGTAGGCGTG	bGH	TAGAAGGCACAGTCGAGG
A4	αoA	CMV	CGCAAATGGGCGGTAGGCGTG	bGH	TAGAAGGCACAGTCGAGG
A5	αoB	CMV	CGCAAATGGGCGGTAGGCGTG	bGH	TAGAAGGCACAGTCGAGG
A6	αz	CMV	CGCAAATGGGCGGTAGGCGTG	bGH	TAGAAGGCACAGTCGAGG
A7	αGust.	CMV	CGCAAATGGGCGGTAGGCGTG	bGH	TAGAAGGCACAGTCGAGG
A8	αsS	CMV	CGCAAATGGGCGGTAGGCGTG	bGH	TAGAAGGCACAGTCGAGG
A9	αsL	CMV	CGCAAATGGGCGGTAGGCGTG	bGH	TAGAAGGCACAGTCGAGG
A10	αQ	CMV	CGCAAATGGGCGGTAGGCGTG	bGH	TAGAAGGCACAGTCGAGG
A11	α11	CMV	CGCAAATGGGCGGTAGGCGTG	bGH	TAGAAGGCACAGTCGAGG
A12	α15	CMV	CGCAAATGGGCGGTAGGCGTG	bGH	TAGAAGGCACAGTCGAGG
B1	α12	CMV	CGCAAATGGGCGGTAGGCGTG	bGH	TAGAAGGCACAGTCGAGG
B2	α13	CMV	CGCAAATGGGCGGTAGGCGTG	bGH	TAGAAGGCACAGTCGAGG
B3	β1	T7	TAATACGACTCACTATAGGG	bGH	TAGAAGGCACAGTCGAGG
B4	β3	T7	TAATACGACTCACTATAGGG	bGH	TAGAAGGCACAGTCGAGG
B5	γ1	T7	TAATACGACTCACTATAGGG	bGH	TAGAAGGCACAGTCGAGG
B6	γ8	T7	TAATACGACTCACTATAGGG	bGH	TAGAAGGCACAGTCGAGG
B7	γ9	T7	TAATACGACTCACTATAGGG	bGH	TAGAAGGCACAGTCGAGG
B8	γ13	T7	TAATACGACTCACTATAGGG	bGH	TAGAAGGCACAGTCGAGG

Declaration of receptors and their respective agonists used

Table C. Declaration of receptors used and their manufacturer.

Receptor abbreviation	Receptor full name	Receptor reference	Agonist	Agonist reference
M1R	Muscarinic M1 receptor	Origene – RC205794	Carbachol	Merck – CAS:51-83-2
D2R	Dopamine receptor 2	Origene – RC202476	Dopamine hydrochloride	Sigma – CAS: 62-31-7
hNTSR1	Human neurotensin receptor 1	Origene – RC220548	Neurotensin	Merck – CAS:60482-95-3
hGPR91	Human G protein receptor 91	Origene - RC205888	Succinic acid disodium salt/Succinate	Sigma - CAS:150-90-3 (99 %)
mGPR91	Murine G protein receptor 91	Origene - MR204545	Succinic acid disodium salt/Succinate	Sigma - CAS:150-90-3 (99 %)

TRUPATH construct combinations

Table D. Declaration of TRUPATH construct combinations used for transfection. These combinations are the ones stated to be the best by Olsen et. al., 2020. Results for cursive constructs are not shown.

α-subunit	β-subunit	γ-subunit
αi1	β3	γ9
αi2	β3	γ8
αi3	β3	γ9
αoA	β3	γ8
αoB	β3	γ8
αz	β3	γ1
aGust	*β3*	*γ1*
asS	*β3*	*γ9*
asL	*β1*	*γ1*
αQ	β3	γ9
α11	β3	γ13
α15	β3	γ13
a12	*β3*	*γ9*
a13	*β3*	*γ9*

Table E. Declaration of sequences used for sequence alignments.

α-subunit	UniProt entry name	UniProt identifier	FASTA sequence
αi1	GNAI1_HUMAN	P63096	MGCTLSAEDKAAVERSKMIDRNLREDGEKAAREVKLLLLGAGESGKSTIVKQMKIIHEAG YSEEECKQYKAVVYSNTIQSIIAIIRAMGRLKIDFGDSARADDARQLFVLAGAAEEGFMT AELAGVIKRLWKDSGVQACFNRSREYQLNDSAAYYLNDLDRIAQPNYIPTQQDVLRTRVK TTGIVETHFTFKDLHFKMFDVGGQRSERKKWIHCFEGVTAIIFCVALSDYDLVLAEDEEM NRMHESMKLFDSICNNKWFTDTSIILFLNKKDLFEEKIKKSPLTICYPEYAGSNTYEEAA AYIQCQFEDLNKRKDTKEIYTHFTCATDTKNVQFVFDAVTDVIIKNNLKDCGLF
αi2	GNAI2_HUMAN	P04899	MGCTVSAEDKAAAERSKMIDKNLREDGEKAAREVKLLLLGAGESGKSTIVKQMKIIHEDG YSEEECRQYRAVVYSNTIQSIMAIVKAMGNLQIDFADPSRADDARQLFALSCTAEEQGVL PDDLSGVIRRLWADHGVQACFGRSREYQLNDSAAYYLNDLERIAQSDYIPTQQDVLRTRV KTTGIVETHFTFKDLHFKMFDVGGQRSERKKWIHCFEGVTAIIFCVALSAYDLVLAEDEE MNRMHESMKLFDSICNNKWFTDTSIILFLNKKDLFEEKITHSPLTICFPEYTGANKYDEA ASYIQSKFEDLNKRKDTKEIYTHFTCATDTKNVQFVFDAVTDVIIKNNLKDCGLF
αi3	GNAI3_HUMAN	P08754	MGCTLSAEDKAAVERSKMIDRNLREDGEKAAKEVKLLLLGAGESGKSTIVKQMKIIHEDG YSEDECKQYKVVVYSNTIQSIIAIIRAMGRLKIDFGEAARADDARQLFVLAGSAEEGVMT PELAGVIKRLWRDGGVQACFSRSREYQLNDSASYYLNDLDRISQSNYIPTQQDVLRTRVK TTGIVETHFTFKDLYFKMFDVGGQRSERKKWIHCFEGVTAIIFCVALSDYDLVLAEDEEM NRMHESMKLFDSICNNKWFTETSIILFLNKKDLFEEKIKRSPLTICYPEYTGSNTYEEAA AYIQCQFEDLNRRKDTKEIYTHFTCATDTKNVQFVFDAVTDVIIKNNLKECGLY
αoA	GNAO_HUMAN (isoform 1)	P09417	MGCTLSAEERAALERSKAIEKNLKEDGISAAKDVKLLLLGAGESGKSTIVKQMKIIHEDG FSGEDVKQYKPVVYSNTIQSLAAIVRAMDTLGIEYGDKERKADAKMVCDVVSRMEDTEPF SAELLSAMMRLWGDSGIQECFNRSREYQLNDSAKYYLDSLDRIGAADYQPTEQDILRTRV KTTGIVETHFTFKNLHFRLFDVGGQRSERKKWIHCFEDVTAIIFCVALSGYDQVLHEDET TNRMHESLMLFDSICNNKFFIDTSIILFLNKKDLFGEKIKKSPLTICFPEYTGPNTYEDA AAYIQAQFESKNRSPNKEIYCHMTCATDTNNIQVVFDAVTDIIIANNLRGCGLY
αoB	GNAO_HUMAN (isoform 2)	P09417	MGCTLSAEERAALERSKAIEKNLKEDGISAAKDVKLLLLGAGESGKSTIVKQMKIIHEDG FSGEDVKQYKPVVYSNTIQSLAAIVRAMDTLGIEYGDKERKADAKMVCDVVSRMEDTEPF SAELLSAMMRLWGDSGIQECFNRSREYQLNDSAKYYLDSLDRIGAADYQPTEQDILRTRV KTTGIVETHFTFKNLHFRLFDVGGQRSERKKWIHCFEDVTAIIFCVALSGYDQVLHEDET TNRMHESLKLFDSICNNKWFTDTSIILFLNKKDIFEEKIKKSPLTICFPEYTGPSAFTEA VAYIQAQYESKNKSAHKEIYTHVTCATDTNNIQFVFDAVTDVIIAKNLRGCGLY
αz	GNAZ_HUMAN	P19086	MGCRQSSEEKEAARRSRRIDRHLRSESQRQRREIKLLLLGTSNSGKSTIVKQMKIIHSGG FNLEACKEYKPLIIYNAIDSLTRIIRALAALRIDFHNPDRAYDAVQLFALTGPAESKGEI TPELLGVMRRLWADPGAQACFSRSSEYHLEDNAAYYLNDLERIAAADYIPTVEDILRSRD MTTGIVENKFTFKELTFKMVDVGGQRSERKKWIHCFEGVTAIIFCVELSGYDLKLYEDNQ TSRMAESLRLFDSICNNNWFINTSLILFLNKKDLLAEKIRRIPLTICFPEYKGQNTYEEA AVYIQRQFEDLNRNKETKEIYSHFTCATDTSNIQFVFDAVTDVIIQNNLKYIGLC

αQ	GNAQ_HUMAN	P50148	MTLESIMACCLSEEAKEARRINDEIERQLRRDKRDARRELKLLLLGTGESGKSTFIKQMR IIHGSGYSDEDKRGFTKLVYQNIFTAMQAMIRAMDTLKIPYKYEHNKAHAQLVREVDVEK VSAFENPYVDAIKSLWNDPGIQECYDRRREYQLSDSTKYYLNDLDRVADPAYLPTQQDVL RVRVPTTGIIEYPFDLQSVIFRMVDVGGQRSERRKWIHCFENVTSIMFLVALSEYDQVLV ESDNENRMEESKALFRTIITYPWFQNSSVILFLNKKDLLEEKIMYSHLVDYFPEYDGPQR DAQAAREFILKMFVDLNPDSDKIIYSHFTCATDTENIRFVFAAVKDTILQLNLKEYNLV
α11	GNA11_HUMAN	P29992	MTLESMMACCLSDEVKESKRINAEIEKQLRRDKRDARRELKLLLLGTGESGKSTFIKQMR IIHGAGYSEEDKRGFTKLVYQNIFTAMQAMIRAMETLKILYKYEQNKANALLIREVDVEK VTTFEHQYVSAIKTLWEDPGIQECYDRRREYQLSDSAKYYLTDVDRIATLGYLPTQQDVL RVRVPTTGIIEYPFDLENIIFRMVDVGGQRSERRKWIHCFENVTSIMFLVALSEYDQVLV ESDNENRMEESKALFRTIITYPWFQNSSVILFLNKKDLLEDKILYSHLVDYFPEFDGPQR DAQAAREFILKMFVDLNPDSDKIIYSHFTCATDTENIRFVFAAVKDTILQLNLKEYNLV
α15	GNA15_HUMAN	P30679	MARSLTWRCCPWCLTEDEKAAARVDQEINRILLEQKKQDRGELKLLLLGPGESGKSTFIK QMRIIHGAGYSEEERKGFRPLVYQNIFVSMRAMIEAMERLQIPFSRPESKHHASLVMSQD PYKVTTFEKRYAAAMQWLWRDAGIRAYYERRREFHLLDSAVYYLSHLERITEEGYVPTAQ DVLRSRMPTTGINEYCFSVQKTNLRIVDVGGQKSERKKWIHCFENVIALIYLASLSEYDQ CLEENNQENRMKESLALFGTILELPWFKSTSVILFLNKTDILEEKIPTSHLATYFPSFQG PKQDAEAAKRFILDMYTRMYTGCVDGPEGSKKGARSRRLFSHYTCATDTQNIRKVFKDVR DSVLARYLDEINLL
GPR91	**UniProt entry name**	**UniProt identifier**	**FASTA sequence**
mGPR91	SUCR1_MOUSE	Q99MT6	MAQNLSCENWLATEAILNKYYLSAFYAIEFIFGLLGNVTVVFGYLFCMKNWNSSNVYLFN LSISDFAFLCTLPILIKSYANDKGTYGDVLCISNRYVLHTNLYTSILFLTFISMDRYLLM KYPFREHFLQKKEFAILISLAVWALVTLEVLPMLTFINSVPKEEGSNCIDYASSGNPEHN LIYSLCLTLLGFLIPLSVMCFFYYKMVVFLKRRSQQQATALPLDKPQRLVVLAVVIFSIL FTPYHIMRNLRIASRLDSWPQGCTQKAIKSIYTLTRPLAFLNSAINPIFYFLMGDHYREM LISKFRQYFKSLTSFRT
hGPR91	SUCR1_HUMAN	Q9BXA5	MLGIMAWNATCKNWLAAEAALEKYYLSIFYGIEFVVGVLGNTIVVYGYIFSLKNWNSSNI YLFNLSVSDLAFLCTLPMLIRSYANGNWIYGDVLCISNRYVLHANLYTSILFLTFISIDR YLIIKYPFREHLLQKKEFAILISLAIWVLVTLELLPILPLINPVITDNGTTCNDFASSGD PNYNLIYSMCLTLLGFLIPLFVMCFFYYKIALFLKQRNRQVATALPLEKPLNLVIMAVVI FSVLFTPYHVMRNVRIASRLGSWKQYQCTQVVINSFYIVTRPLAFLNSVINPVFYFLLGD HFRDMLMNQLRHNFKSLTSFSRWAHELLLSFREK

Results

D2R and hNTSR1 curves

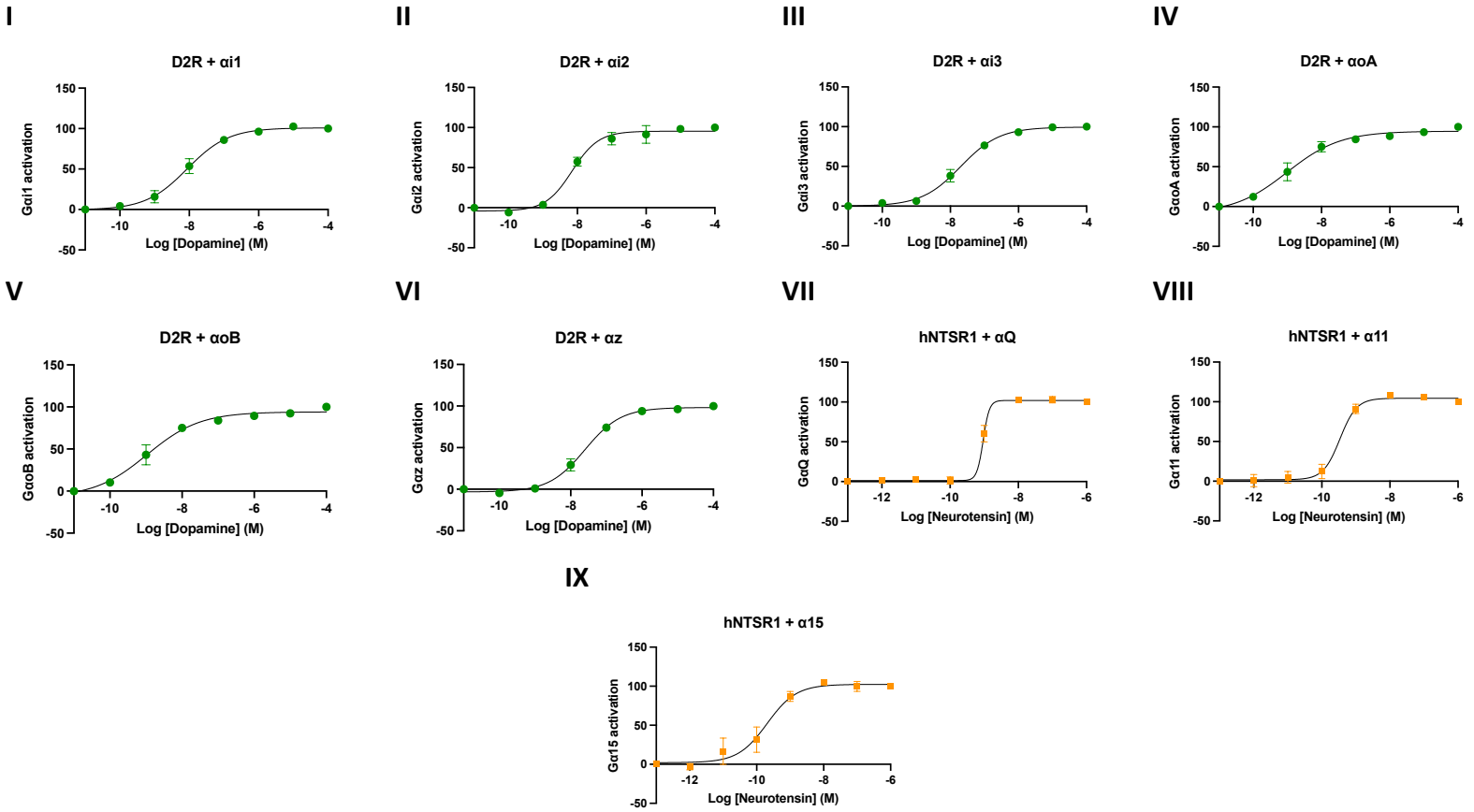

Figure A. I-VI G protein recruitment for D2R (Gi-family). Mean values of N=4, each N consisting of triplicate values ± SEM. D2R recruits all α-subunits in the Gi-family. Log EC50 values: αi1 (A) = -8.1, αi2 (B) = -8.2, αi3 (C) = -7.7, αoA (D) = -9.0, αoB (E) = -9.0, αz (F) = -7.6. **VII-IX** G protein recruitment for hNTSR1 (Gq-family). **VII**, mean values of N=3, each N consisting of triplicates ± SEM. **VIII**, mean values of N=2, each N consisting of triplicates ± SEM. **IX**, mean values of N=5, each N consisting of triplicates ± SEM. hNTSR1 recruits all α-subunits in the Gq-family. Log EC50 values: αQ (G) = -9.0, α11 (H) = -9.5, α15 (I) = -9.7.

EC50 data

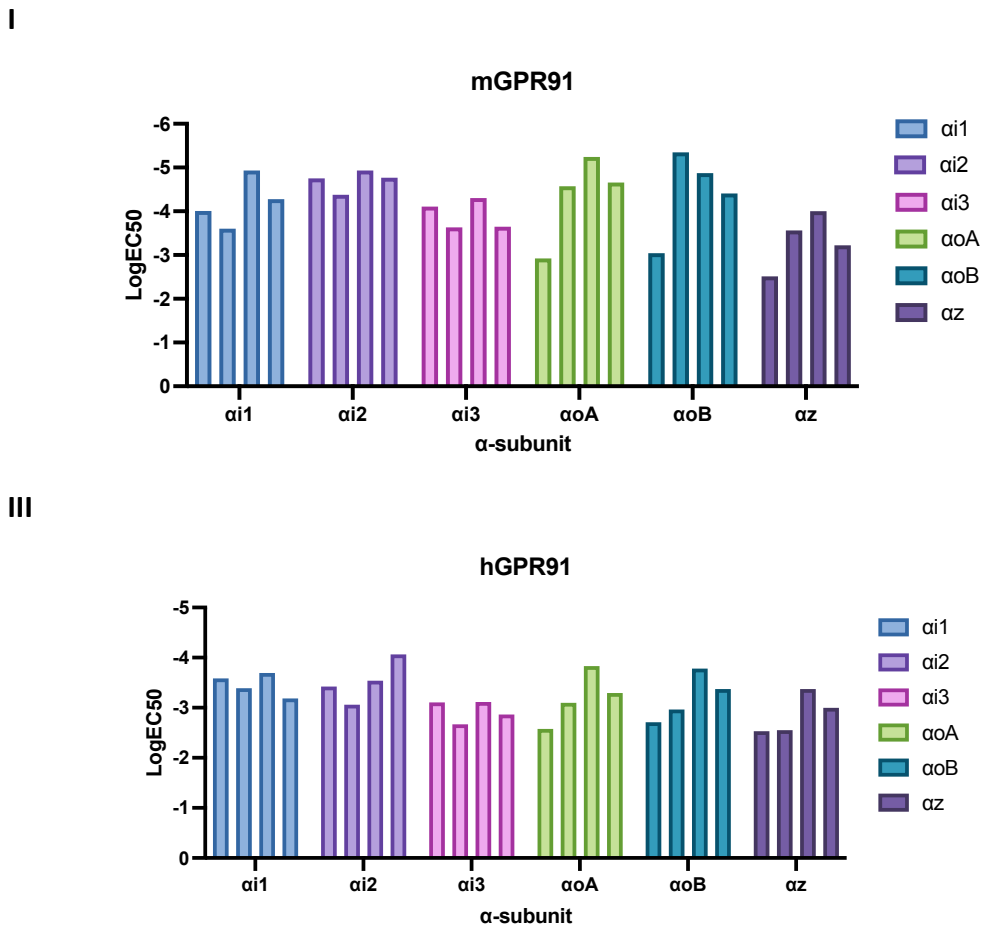

Figure B. I and III, plots of Log EC50 value for each of the four runs for the Gi-family, for mGPR91 (fig. I) and hGPR91 (fig. III). **II and IV**, mean Log EC50 value and + SD for each α-subunit in the Gi-family for mGPR91 (fig. II) and hGPR91 (fig. IV).

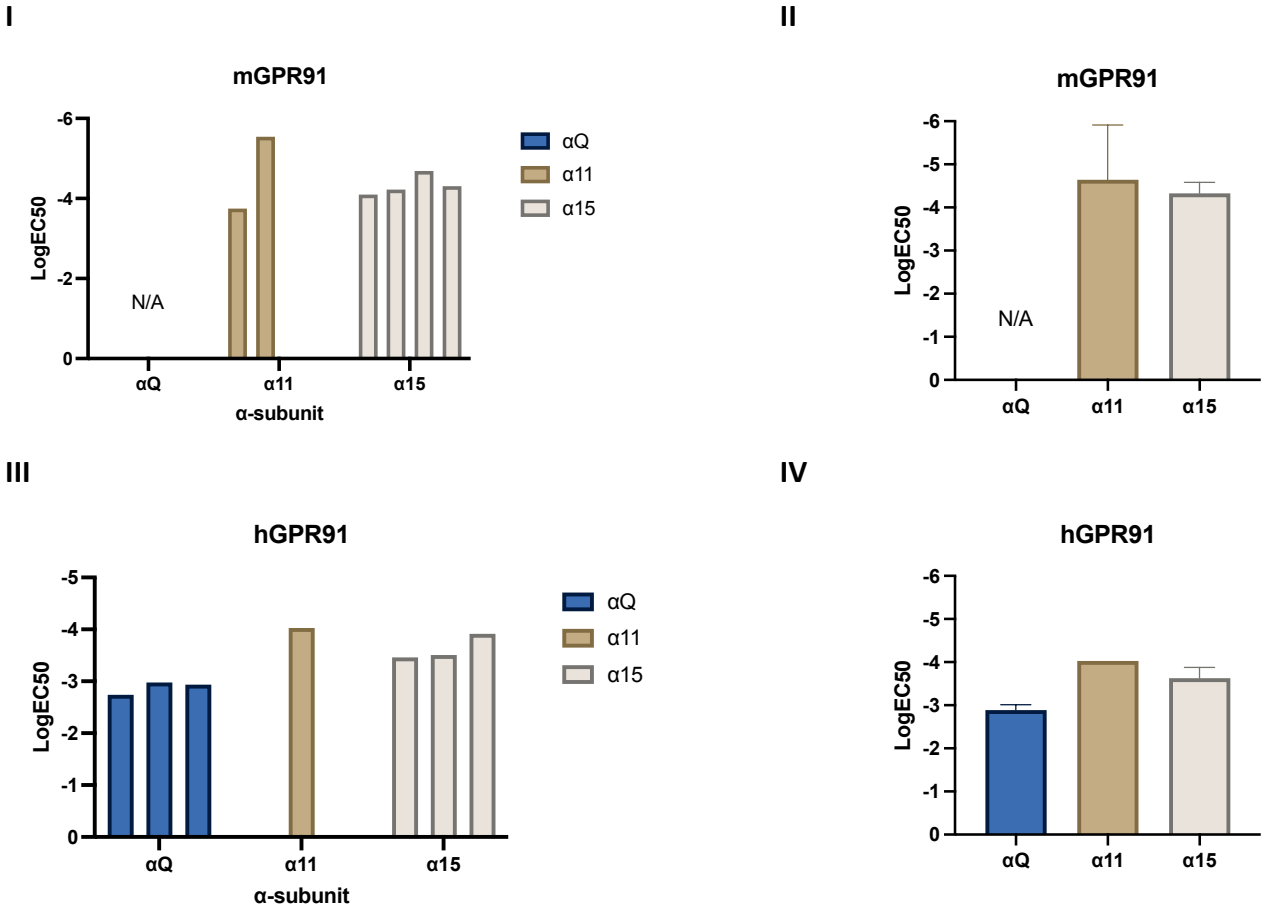

Figure C. I and III, plots of Log EC50 value for each of the runs for the Gq-family, for mGPR91 (fig. I) and hGPR91 (fig. III). **II and IV**, mean Log EC50 value + SD for each α-subunit in the Gq-family for mGPR91 (fig. II) and hGPR91 (fig. IV).

Table F. Log EC50 values for each run that data is presented for, mean Log EC50 and SD. Timepoints from which the data is obtained. Top for mGPR91 and bottom for hGPR91. Crossed out cells mean that there is no data. n/a means that no curves was produced (no recruitment) and thus no EC50 value obtained.

mGPR91	LogEC50				Mean LogEC50	SD	Timepoint from which the data is taken (min)
	run 1	run 2	run 3	run 4			
Gαi-family							
αi1	-4,003	-3,596	-4,929	-4,273	**-4,20025**	*0,5598794*	6/6/6/6
αi2	-4,754	-4,378	-4,933	-4,767	**-4,708**	*0,2346075*	6/6/6/6
αi3	-4,109	-3,633	-4,304	-3,647	**-3,92325**	*0,3366664*	6/6/6/6
αoA	-2,924	-4,572	-5,24	-4,658	**-4,3485**	*0,9949397*	6/6/6/6
αoB	-3,041	-5,347	-4,87	-4,409	**-4,41675**	*0,9939062*	6/6/6/6
αz	-2,513	-3,563	-4,004	-3,224	**-3,326**	*0,6290803*	6/8/6/6
GαQ-family							
αQ	n/a	n/a	n/a	n/a	**n/a**	*n/a*	2/2/2
α11	-3,745	-5,541	~~-4,685~~	~~-4,309~~	**-4,643**	*1,2699638*	6/6
α15	-4,098	-4,224	-4,685	-4,309	**-4,329**	*0,2526671*	6/6/6/6

hGPR91	LogEC50				Mean LogEC50	SD	Timepoint from which the data is taken (min)
	run 1	run 2	run 3	run 4			
Gαi-family							
αi1	-3,586	-3,389	-3,695	-3,187	**-3,46425**	*0,2240526*	6/6/6/6
αi2	-3,422	-3,062	-3,541	-4,063	**-3,522**	*0,4141827*	6/6/6/6
αi3	-3,107	-2,669	-3,115	-2,863	**-2,9385**	*0,2143789*	6/6/6/6
αoA	-2,575	-3,096	-3,832	-3,292	**-3,19875**	*0,519398*	6/6/6/6
αoB	-2,71	-2,965	-3,782	-3,372	**-3,20725**	*0,4702562*	6/8/6/6
αz	-2,531	-2,554	-3,374	-2,996	**-2,86375**	*0,4018759*	6/6/8/6
GαQ-family							
αQ	-2,74	-2,976	-2,935	~~-2,916~~	**-2,88366667**	*0,1260965*	2/2/2
α11	-4,025	~~-3,506~~	~~-3,916~~	~~-2,916~~	**-4,025**	*n/a*	8
α15	-3,461	-3,506	-3,916	~~-2,916~~	**-3,62766667**	*0,2507156*	6/6/6

Sequence alignments

I

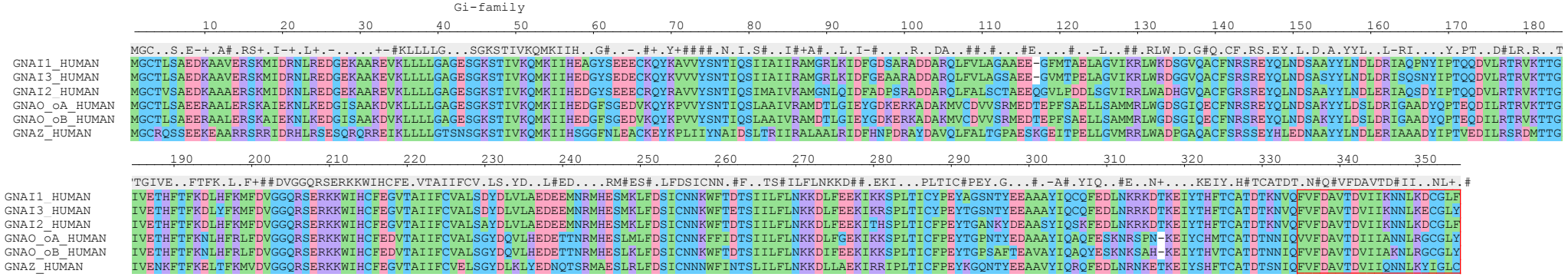

II

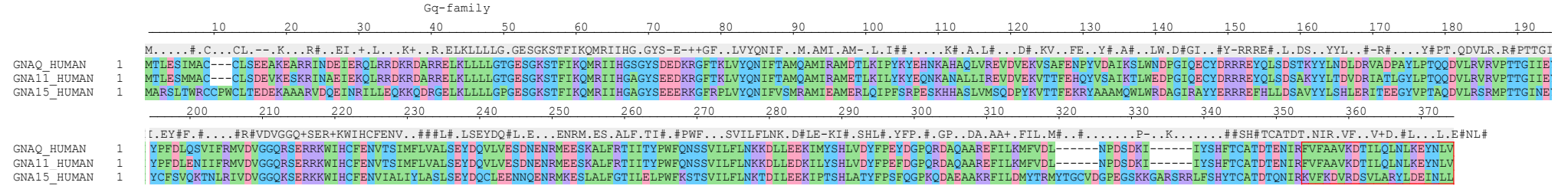

Figure D. Full sequence alignments of the alpha subunits in the Gi-family (fig. I) and Gq-family (fig. II). Colours represent amino acid properties, green - hydrophobic, blue – hydrophilic, pink – acidic and purple – basic. Red squared sequence is investigated further in the results and discussion section as the part of the sequence that interacts with the GPCR

Popular science summary

Better and safer drugs, the importance of understanding how cells talk

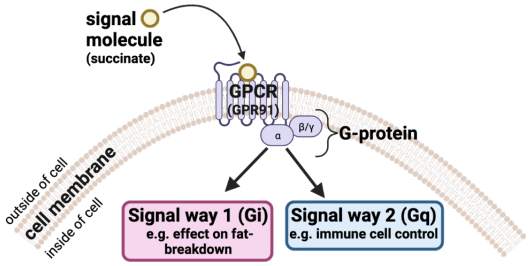

Key ingredients when trying to understand how and why a disease progresses and when eventually finding a treatment or drug is to understand WHAT is happening in the diseased cells and WHY it is happening. Many diseases are a result of signalling within or between cells going wrong. To be able to effectively address the problem one needs to know as much as there is about the root cause. In this thesis its shown that one specific cell-signal-mediator (receptor) can signal in two very different ways, with the same signal-molecule (ligand) that could lead to two separate outcomes.

G protein-coupled receptors (GPCRs) are one of the most common mediators of signalling in cells being involved in everything from hormone and immune signalling to being central parts of our vision, olfaction, and taste. GPCRs are also one of the most common targets for drugs. GPCRs are dependent on G proteins to bind to them on the inside of the cell and are the ones that further signals in the cell. For the G-protein to bind to the GPCR it must be called upon from the outside of the cell by a signal molecule. There are four main types of G proteins that can bind to the receptor, resulting in 4 different signal ways. We have shown that the succinate receptor 1 (SUCNR1/GPR91) that is one of the approximately 800 GPCRs we have in our cells, is able to bind two different types of G proteins (called Gi and Gq), which as mentioned, eventually can lead to different cellular outcomes. We also show that GPR91 binds more consistently and more strongly to one (Gi) over the other (Gq). The reason for the receptor's preference towards Gi is not entirely known, but we do know that Gi and Gq have differences to their structures, which would affect how and how strongly it can bind to the receptor. We also compared the succinate receptor from mouse with the one from human. Here we observed that the mouse-receptor needed, in general, less signal molecules to call the two different G proteins than what the human-receptor needed. Why this is, is also not known, but as for the different G proteins, the mouse and human receptor have structural differences that could affect how it binds the signal molecule and then how it interacts with the G protein. So again, why is this knowledge important? Giving the example of the investigated succinate receptor (GPR91) we know that it takes part in signalling in many different tissues (e.g., liver, brain, heart, and kidney) and are involved in different diseases in these tissues. So, if we can predict and control the behaviour of GPCRs that as mentioned are very common drug targets, we can design more precise and efficacious drugs that in the end will also result in less side effects which is very desirable. How do we now move forward with this knowledge? Now that we know that GPR91 can signal with two different G proteins we want to know what is controlling the behaviour. Can we find a signal molecule that affects GPR91 to choose one signal way over the other? Can we attribute a signal way to specific locations in the body? These are questions to be answered in the future. And the answers will lead drug discovery and development forward.

Populärvetenskaplig sammanfattning

Bättre och säkrare läkemedel, vikten av att förstå hur våra celler kommunicerar

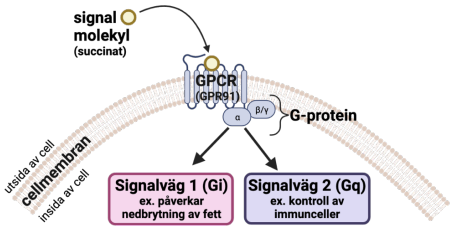

När man ska börja försöka förstå varför en sjukdom utvecklas och sprider sig, eller när man ska uppfinna ett nytt läkemedel är det första steget att förstå VAD som händer i dom sjuka cellerna och VARFÖR det händer. Många sjukdomar är ett resultat av när signalering i eller mellan celler går fel. För att man så effektivt som möjligt ska kunna adressera problemet behöver man alltså veta så mycket som möjligt om ursprunget till sjukdomen. I denna avhandling visar vi att en viss cell-kommunikatör (receptor) kan signalera på två olika sätt med samma signal-molekyl (ligand), som slutligen leder till två olika händelser inuti cellen.

G-proteinkopplade receptorer (GPCRs) är en av de vanligaste förmedlarna av signalering i celler som är involverade i allt från hormon- och immunsignalering till att vara centrala delar av vår syn, lukt och smak. GPCRs är också ett av de vanligaste målen för läkemedel. GPCRs är beroende av G-proteiner för att binda till dem på insidan av cellen och är de som signalerar vidare i cellen. För att G-proteinet ska binda till GPCRs måste det anropas från utsidan av cellen av en signalmolekyl. Det finns fyra huvudtyper av G-proteiner som kan binda till receptorn, vilket resulterar i fyra olika signalvägar. Vi har visat att succinatreceptorn 1 (SUCNR1/GPR91) som är en av de cirka 800 GPCRs vi har i våra celler, kan binda två olika typer av G-proteiner (kallade Gi och Gq), som nämnts så småningom kan leda till olika cellulära utfall. Vi visar också att GPR91 binder mer konsekvent och starkare till den ena (Gi) än den andra (Gq). Orsaken till receptorns preferens för Gi är inte helt känd, men vi vet att Gi och Gq har skillnader i sina strukturer, vilket skulle påverka hur och hur starkt det kan binda till receptorn. Vi jämförde också succinatreceptorn från mus med den från människa. Här observerade vi att musreceptorn i allmänhet behövde mindre signalmolekyler för att rekrytera de två olika G-proteinerna än vad den mänskliga receptorn behövde. Varför detta är, är inte heller känt, men vad gäller de olika G-proteinerna så har mus- och humanreceptorn strukturella skillnader som kan påverka hur den binder signalmolekylen och sedan hur den interagerar med G-proteinet. Så återigen, varför är denna kunskap viktig? Med exemplet med den undersökta succinatreceptorn (GPR91) vet vi att den deltar i signalering i många olika vävnader (t.ex. lever, hjärna, hjärta och njure) och är involverad i olika sjukdomar i dessa vävnader. Så om vi kan förutsäga och kontrollera beteendet hos GPCRs som nämnts är mycket vanliga läkemedelsmål, kan vi designa mer exakta och effektiva läkemedel som i slutändan också kommer att resultera i färre biverkningar vilket är mycket önskvärt. Hur går vi nu vidare med denna kunskap? Nu när vi vet att GPR91 kan signalera med två olika G-proteiner vill vi veta vad som styr beteendet. Kan vi hitta en signalmolekyl som påverkar GPR91 för att välja en signalväg framför den andra? Kan vi tillskriva en signalväg till specifika platser i kroppen? Det är frågor som ska besvaras i framtiden. Och svaren kommer att leda läkemedelsutvecklingen framåt.